Design and Manufacture Study of Ocean Renewable Energy Storage (ORES) Prototype

by

Gökhan Dündar

B.S. Mechanical Engineering
Turkish Naval Academy, 2006

Submitted to the Department of Mechanical Engineering
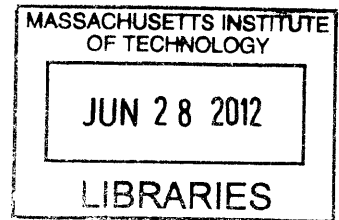in partial fulfillment of the requirement for the degree of

Master of Science in Mechanical Engineering

at the

Massachusetts Institute of Technology

June 2012

Signature of Author:

Department of Mechanical Engineering
11 May 2012

Certified by:

Alexander H. Slocum
Pappalardo Professor of Mechanical Engineering
Thesis Supervisor

Accepted by:

David E. Hardt
Ralph E. and Eloise F. Cross Professor of Mechanical Engineering
Chairman, Committee for Graduate Students

"Hayatta en hakiki mürşit ilimdir, fendir."

Mustafa Kemal Atatürk

Design and Manufacture Study of Ocean Renewable Energy Storage (ORES) Prototype

By

Gökhan Dündar

Submitted to the Department of Mechanical Engineering
on May 11, 2012 in Partial Fulfillment of the Requirements for
the Degree of Master of Science in
Mechanical Engineering

Abstract

Utility scale energy storage is needed to balance rapidly varying outputs from renewable energy systems such as wind and solar. In order to address this need, an innovative utility scale energy storage concept has been created by the Precision Engineering Research Group (PERG) at MIT. The concept is to build hollow concrete structures to act as lower reservoir, install pump/turbine units, deploy them under the ocean and use the hydrostatic pressure of the water column as an upper reservoir to run the turbine and generate electricity, and pump the water out of the structure to store energy. The result is similar to a conventional Pumped Storage Hydroelectric (PSH) facility that operates on land using lakes and dams.

Evolution of the ORES project will be presented and design iterations discussed in detail. Each design option is evaluated to better understand advantages and disadvantages. Concrete related tests were conducted to develop manufacturing process and evolve design assumptions. Global sites are evaluated for ORES deployment including an intensive study on the Mediterranean and Japan.

Our research shows that storing energy underwater is technically and economically feasible and has great potential. Our geographical evaluations show that the Gulf of Maine, off coast of California, Hawaii, Mediterranean and Japan have great potential for both wind and ocean depths that favor ORES deployment.

Thesis Supervisor   : Alexander H. Slocum
Title   : Pappalardo Professor of Mechanical Engineering

[Left Blank]

Acknowledgements

I hereby want to acknowledge:

- My advisor Prof Alex Slocum for his insights with the project, ability to solve design and engineering problems and continuous support during my life at MIT. He is not only a professor but more than that a role model, a mentor and a sportsman. Thank you for your guidance and hospitality. I hope to see you in Turkey for a diving trip!

- Turkish Navy for financially supporting me during my education. I had two childhood dreams, being an officer and coming to MIT. Thank you for making this possible. I am very proud of being a Turkish Naval Officer.

- Brian Hodder, for his friendship, hospitality and ability to look at the project from a broader perspective. He also had continuous support during my masters and made this experience unique for me. Thank you for editing and challenging my thesis.

- Gregory Fennell, James Meredith it was a pleasure to work with you. Elie Homsi from Flatiron, Christoph Lay and Andreas Garg from Hochtief for their continuous input and bringing up solutions to the project challenges. Nevan Hanumara, Folkers Rojas and my lab mates, Precision Engineering Research Group. We established such a concrete relationship. It was a pleasure to meet and work with you.

- My great family, my mother Sevgi, my father Mustafa and brother Özgür. I am very lucky for having such a loving and caring family. This wouldn't be possible without your continuous support and ability to calm me down. Your guidance enlightened my way.

- And finally my fiancé Emine. I am sorry for being away from you for two years but I hope this will enforce our relationship and provide us better opportunities in the future. Thank you for your continuous support. You are the reason for me to stick to my goal.

[Left Blank]

Table of Contents

List of Figures

9

List of Tables

Nomenclature

Variable	Unit	Description
h	m	Head. Height of water column.
η		Eta. Efficiency
ρ	kg/m^3	Density
D	m	Diameter
R	m	Outer radius
r	m	Radius
FoS		Factor of Safety
t	m	Wall thickness
E	Joules	Energy (unless otherwise stated)
kW	W	Kilowatt
MW	W	Megawatt
MWh	Wh	Megawatt-hour
mt		Metric tonne
Psi		Pound per square inch
Pa	N/m^2	Pascals
kPa	1E3 Pa	Kilopascal
MPa	1E6 Pa	Megapascals
W	mt	Weight
V	m^3	Volume
NM		Nautical miles (1852m)
α	K^{-1}	Coefficient of thermal expansion
μ	Pa.s	Viscosity
P	Pa	Pressure
T	Kelvin	Temperature
g	m/s^2	Gravitational acceleration
A	m^2	Area
L	m	Length
σ	Pa	Stress
F	N	Force

[Left Blank]

Chp.1   Introduction

1.1. Motivation

Demand for energy has been growing rapidly and is projected to continue increasing in the 21th century. Due to increasing oil prices, political instability on the supply side, need for a higher quality grid and rising environmental concerns more and more renewable energy is being installed. Wind followed by solar PV are the two major sources which accounts for 84% of global renewable investment in 2010 [1]. However these technologies, particularly wind, bring problems. As a result of the uncontrollable character of these resources, the biggest challenge is the mismatch between the energy generated and the demand.

Recent studies on offshore wind show that better wind profiles exist and higher capacity factors can be achieved farther offshore [2]. There have been numerous studies on Floating Wind Turbines (FWTs) to exploit higher winds offshore. Even though higher winds can be utilized with proposed technologies, an energy storage capability will increase the real value of offshore wind. Furthermore these technologies will require anchors to stay in their projected places. Two different anchorage systems are envisioned to be used depending on the application, catenary mooring or Tension Leg Platform (TLP). Each of the anchoring system will have different requirements.

In order to address two major challenges for the offshore wind a utility scale energy storage project, Ocean Renewable Energy Storage (ORES) is developed as the focus of this thesis. Made from concrete, these structures can store energy for offshore wind for future use and can be connected to FWTs to meet the requirements for anchorage systems. While providing storage to increase the value of the renewable energy, the ORES system can also serve as anchorage systems thus share costs to reduce total system cost.

1.2. Thesis Outline

Chapter 2 will primarily discuss about need for energy storage and introduce utility scale energy storage technologies. In addition to commercially viable applications, innovative approaches and recent studies are going to be discussed in detail.

Chapter 3 is going to review evolution of ORES project, design features, calculations, simulations and analysis.

Chapter 4 is going to analyze cylindrical tubes as an alternative geometry to the current spherical approach. Capacity and volume calculations will be presented and compared to spherical approach.

Chapter 5 will provide information about research we have done related to concrete, test results, experience gained and lessons learned.

Chapter 6 will present possible deployment sites around globe will discuss in detail and preliminary analysis of sites.

In conclusion lessons learned will be summarized and next steps will be proposed for the ORES project.

Chp 2.   Need for Energy Storage

Utility scale energy storage is essential for various reasons primarily, load leveling, frequency regulations and transmission deferral. Power plants are dispatched according to merit order. Coal and nuclear plants from conventional sources and hydroelectric, geothermal, biomass and solar thermal with energy storage, from renewable sources are technologies which act as baseload plants. Baseload plants are used to satisfy the minimum continuous energy demand of a specific demand center. They can operate almost entire year and are stopped only because of maintenance. These plants have a long ramp-up time, which means they require long time to operate in their highest design efficiencies. Baseload plants operate in their most efficient output and generate constant power output thus electricity produced from these plants is relatively cheaper to other energy generating plants. Since these plants are designed to meet constant demand throughout the year and do not meet the instant demand changes additional power plants are required to meet the changing demand in the grid.

Intermediate plants, also known as load following power plants, are dispatched to meet the extra demand on the grid which baseload plants cannot satisfy. They have faster ramp-up times compared to baseload plants and can be operational within minutes to hours. Depending on the technology they can operate for long periods like baseload plants however are not designed to run almost during the entire year. Boiling Water Reactors (BWR), steam turbines, some of the gas turbines and hydroelectric plants are examples of intermediate plants. They start generating electricity hours before expected demand increase (i.e. before air conditioning makes peak) and stop after demand decreases. These plants are usually turned on and off daily to meet daily demands. However additional fast ramp-up power plants are required to meet peak demands.

Peak power plants, also known as peaker plants, are designed to meet only the peak demand. They are dispatched in cases where baseload plants and intermediate plants are operational yet cannot satisfy the peak demand. Even though these plants are used very rarely they are required in case of unpredicted spikes in the demand. 10% of the total electricity generating capacity, which is the peaker plants, is used only 50 hours a year [3]. Natural Gas (NG) turbines are generally used to meet the peak demand. They have very short ramp-up times and can be fully operational and synchronized with the grid within minutes. They are dispatched only to meet the peak demand and are turned off after demand is satisfied. The cost of electricity which peak plants produce is higher than intermediate and baseload plants.

Different levels of power plants are dispatched to meet the demand thus the price of electricity will be strongly correlated to demand. Utilities would use load leveling (a.k.a. peak-shaving) to store cheap energy from the baseload plants primarily, coal and nuclear plants, during off-peak times and release it when there is high demand and prices are high. Storage also

reduces the need for short-ramping-time expensive NG turbines. Dispatchability profile by power plants is shown in Figure 1.
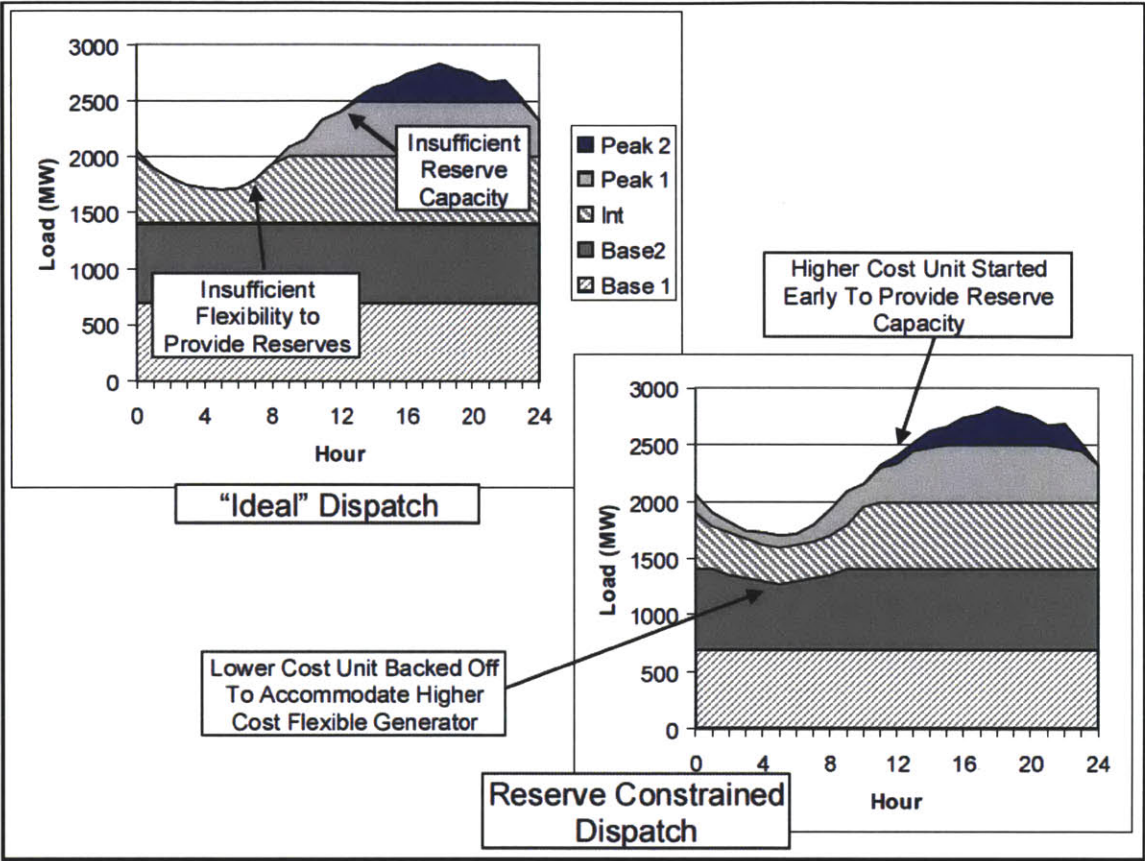
Figure 1 Dispatch profile of power plants [4]

Energy price corresponding to dispatched plants is shown in Figure 2. Figure 1 shows that the peak demand at 18.00 is satisfied by dispatching all baseload plants, intermediate plants and peaker plants, and the corresponding electricity price is also at a peak Figure 2.

Figure 2 Electricity price at Node MURRAY_6_N015 for February 13th, 2011[5]

In order to lower the electricity price at peak times, cheap energy produced by baseload plants or renewables; namely wind, geothermal, tidal and current, during the off-peak times is stored in either PSH, CAES or advanced batteries in utility scale. A typical schematic for load leveling can be seen in Figure 3.
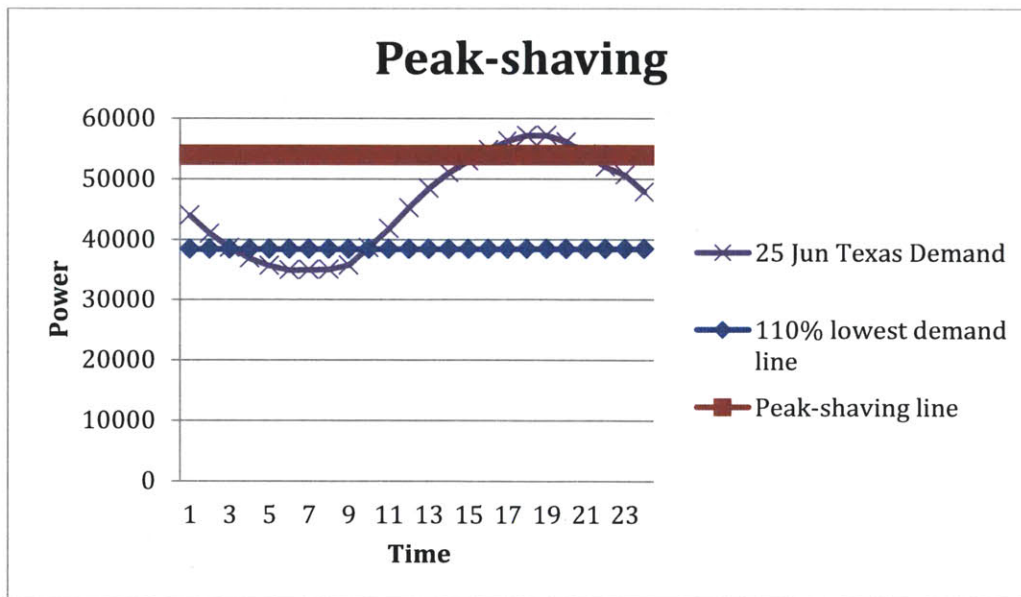
Figure 3 Graph of typical load-leveling (a.k.a. peak-shaving)

Another reason for storage is transmission deferral. Transmission line installations are very expensive and are subject to strict and complicated legal permitting. In addition depending on the location and coverage of the project it can be bound by multiple states legislations as well as federal legislations. Even though there have been numerous studies on transmission line installations there is not a universal agreement on absolute cost of transmission lines due to the

18

high number of variables. Most of this variation is highly because of different types (underwater, AC or DC) and various capacities (800kV, 765kV, 500kV, 345kV, 230kV and 115kV) of the lines. An extensive research conducted by Lawrence Berkeley National Laboratories shows that the cost for transmission lines range from $0.3-$2 million/mile [6]. The result of the study can be seen in Table 1.

Table 1 Types, capacity and cost of transmission lines (source:[6]) (all costs are $million/mi unless otherwise stated)

Transmission Lines	Minimum Cost	Average Cost	Maximum Cost	Number of Samples
765 kV (no description)	2.0		3.2	5
500 kV (single circuit)	1.5		2.2	6
500 kV (double circuit)	2.0		3.5	5
500 kV (no description)	0.8		2.6	10
HVDC Line (800kV)		3.7		1
HVDC Line (345 - 500kV)	1.1		3.0	8
HVDC Undersea Cable		4.0		1
345 kV (single circuit)	0.6		1.5	4
345 kV (double circuit)	1.0		2.3	5
345 kV (no description)	0.5		2.2	10
230 kV (double circuit)		2.0		1
230 kV (no description)	0.3		1.6	6
230 kV (rebuild/reconductor)		0.5		1
115 kV (no description)	0.2		0.4	2
115kV (rebuild/reconductor)	0.1		0.3	2
115 kV (uprate)	0.05		0.4	2
Associated Equipment				
HV Substations ($/unit)	10		60	6
DC Terminal ($/MW)	0.1		0.2	4
DC Terminal ($/unit)	250		500	5

If there is a transmission bottleneck a solution is to build more transmission lines. Instead of building costly transmission lines the problem can also be addressed by building a storage device on the demand side of the bottleneck. Therefore when demand exceeds the transmission capacity stored energy is released to satisfy the demand. An additional solution is "Demand

Response" (DR). When demand approaches critical levels and energy price spikes, consumers are encouraged to reduce their energy consumptions to decrease peak price and mitigate grid response problems. Customers are then compensated according to the reduction they make during the peak times. Even though these approaches are very innovative and a part of smart grid these scenarios are out the scope of this project and will not be discussed in detail.

The third reason for utility scale energy storage is efficient integration of higher levels of renewable energy, particularly wind power. The main disadvantage of intermittent renewable energy technologies, solar PV, solar thermal, wind, wave current and tidal, is the fact that there is a mismatch between demand and supply as demand is consistent according to diurnal and seasonal changes (peak in summer and afternoons) but supply (wind, wave) is dependent upon uncontrollable natural forces. Furthermore these power plants are not dispatchable. The intermittency problem can be answered by having spinning reserves connected to and synchronized with the grid and fast ramping power plants such as Advanced NG. However without a proper storage technology non-dispatchability of aforementioned energy resources remains still. Installing sufficient storage will increase the real value of renewables and allow them to be used in case of need. This supplementary capability can make a difference in the energy industry. Table 2 summarizes an extensive study conducted by national renewable energy laboratory which reveals the value of storage with respect to corresponding purposes [7].

Table 2 Economic benefits of energy storage [7]

#	Benefit Type	Discharge Duration*		Capacity (Power: kW, MW)		Benefit ($/kW)**		Potential (MW, 10 Years)		Economy ($Million)†	
		Low	High	Low	High	Low	High	CA	U.S.	CA	U.S.
1	Electric Energy Time-shift	2	8	1 MW	500 MW	400	700	1,445	18,417	795	10,129
2	Electric Supply Capacity	4	6	1 MW	500 MW	359	710	1,445	18,417	772	9,838
3	Load Following	2	4	1 MW	500 MW	600	1,000	2,889	36,834	2,312	29,467
4	Area Regulation	15 min.	30 min.	1 MW	40 MW	785	2,010	80	1,012	112	1,415
5	Electric Supply Reserve Capacity	1	2	1 MW	500 MW	57	225	636	5,986	90	844
6	Voltage Support	15 min.	1	1 MW	10 MW	400		722	9,209	433	5,525
7	Transmission Support	2 sec.	5 sec.	10 MW	100 MW	192		1,084	13,813	208	2,646
8	Transmission Congestion Relief	3	6	1 MW	100 MW	31	141	2,889	36,834	248	3,168
9.1	T&D Upgrade Deferral 50th percentile††	3	6	250 kW	5 MW	481	687	386	4,986	226	2,912
9.2	T&D Upgrade Deferral 90th percentile††	3	6	250 kW	2 MW	759	1,079	77	997	71	916
10	Substation On-site Power	8	16	1.5 kW	5 kW	1,800	3,000	20	250	47	600
11	Time-of-use Energy Cost Management	4	6	1 kW	1 MW	1,226		5,038	64,228	6,177	78,743
12	Demand Charge Management	5	11	50 kW	10 MW	582		2,519	32,111	1,466	18,695
13	Electric Service Reliability	5 min.	1	0.2 kW	10 MW	359	978	722	9,209	483	6,154
14	Electric Service Power Quality	10 sec.	1 min.	0.2 kW	10 MW	359	978	722	9,209	483	6,154
15	Renewables Energy Time-shift	3	5	1 kW	500 MW	233	389	2,889	36,834	899	11,455
16	Renewables Capacity Firming	2	4	1 kW	500 MW	709	915	2,889	36,834	2,346	29,909
17.1	Wind Generation Grid Integration, Short Duration	10 sec.	15 min.	0.2 kW	500 MW	500	1,000	181	2,302	135	1,727
17.2	Wind Generation Grid Integration, Long Duration	1	6	0.2 kW	500 MW	100	782	1,445	18,417	637	8,122

*Hours unless indicated otherwise. min. = minutes. sec. = seconds.
**Lifecycle, 10 years, 2.5% escalation, 10.0% discount rate.
†Based on potential (MW, 10 years) times average of low and high benefit ($/kW).
†† Benefit for one year. However, storage could be used at more than one location at different times for similar benefits.

In order to mitigate the risk and effects of allowing more renewables in the current energy portfolio different kinds of energy storage technologies are used. Pumped Storage Hydroelectric (PSH) and Compressed Air Energy Storage (CAES) are used to address utility scale energy storage needs. Fly-wheels and Electric Double-Layer Capacitors (EDLC) are used for improving grid power quality while high capacity batteries are used for the operations in between. Energy storage technologies used for different purposes with respect to their energy storage capacities and discharge rates are shown in Figure 4.
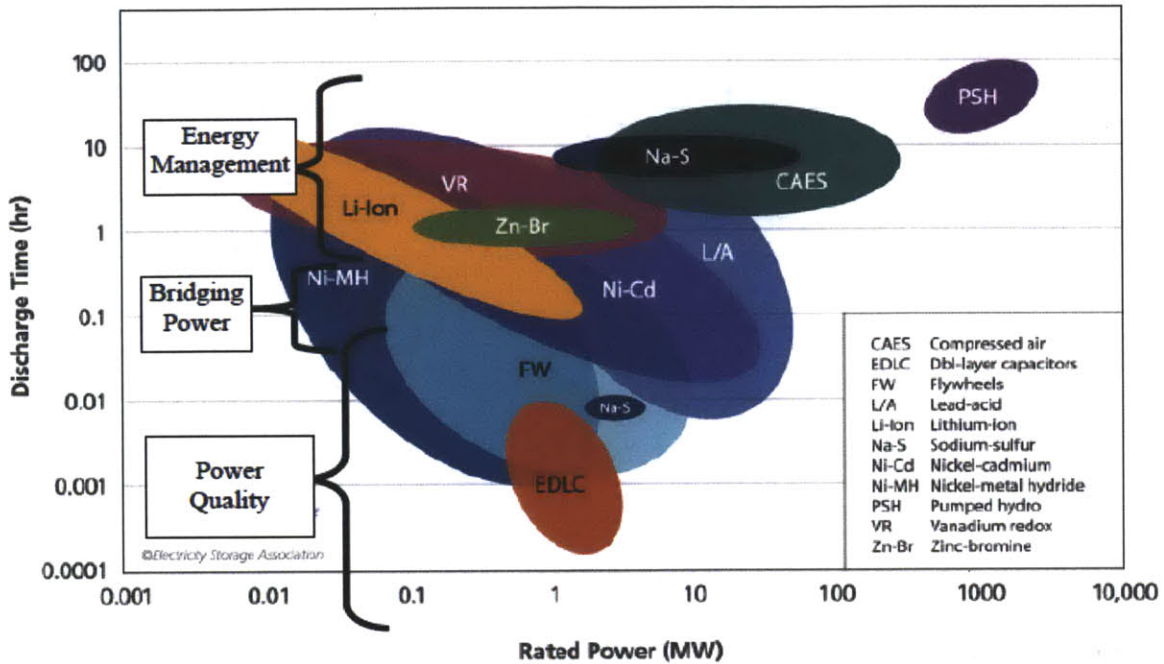
Figure 4 Energy storage technologies with respect to their storage capacities and discharge rates (Source:[8]) [7]

Power quality management and bridging powers are outside the scope of this project. This paper will focus on energy management storage solutions, which are served by utility scale energy storage. For the purpose of this paper energy storage will refer to utility scale energy storage.

2.1. Energy Storage Technologies

2.1.1. Pumped Storage Hydroelectric (PSH)

PSH is the most common and well-proven energy storage technology which utilizes the head difference between two reservoirs. During low-demand (off-peak) times water is pumped from a lower reservoir to an upper reservoir. When power is needed, water is released to flow down to the lower reservoir through a turbine to generate electricity. A schematic of PSH in Racoon Mountain Pumped Storage Plant is shown in Figure 5.
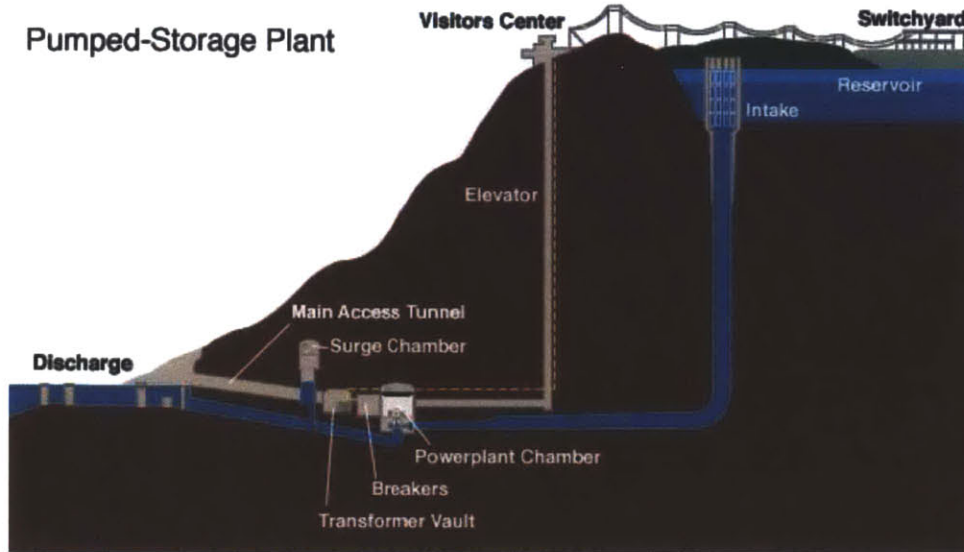
Figure 5 Diagram of Raccoon mountain Pumped Storage Plant (http://www.tva.gov/power/pumpstorart.htm)

Essentially electrical energy is converted to, and stored as, potential energy. Energy capacity of the system is proportional to the head difference between the reservoirs and volume of the upper reservoir. The energy capacity of the system can be calculated as:

$$E = \rho_{water} \times g \times h \times V_{reservoir} \times \eta_{pump} \times \eta_{turbine} \tag{1}$$

Compared to other energy storage technologies PSH is the oldest and most well-established technology. PSH was first commercially built back in 1890s in Italy and Switzerland and has been widely used since then. Currently led by Japan, worldwide PSH installed capacity is 104,453 GWh [9]. Table 3 represents worldwide PSH capacity by countries.

Table 3 Installed PSH capacity of EU countries [10], US [11], China [12] and Japan [13]

Country	Installed PSH Nameplate Capacity (MW)
Japan	25,583
USA	21,886
China	15,643
Italy	7,544
Spain	5,347
Germany	5,223
France	4,303
Austria	3,580
United Kingdom	2,744
Switzerland	1,655
Poland	1,406
Belgium	1,307
Czech Republic	1,147
Luxemburg	1,100
Portugal	1,029
Slovakia	916
Bulgaria	864
Latvia	760
Greece	699
Croatia	293
Ireland	292
Sweden	45

2.1.2.   Compressed Air Energy Storage (CAES)

As its name suggests; CAES stores energy using compressed air; energy is then released by using the compressed air to spin a turbine. For conventional CAES, power is drawn from the grid off-peak to compress air, and delivered to the grid on-peak by expanding the air through a turbine. When the system is charged during compression, the air heats up, and that heat is dissipated to the environment. Since thermal energy during the compression stage is not stored in the existing systems, efficiency and capacity drops due to entropy generation. In order to compensate the losses, natural gas (NG) is combusted with the compressed air during discharge, and the combustion product is used to drive a turbine. Geological features, such as depleted underground salt caverns, are required with the current applications therefore both worldwide and domestic CAES installations are highly restricted geographically. Regions in Europe and US that can support conventional CAES are shown in Figure 6 and Figure 7 respectively.
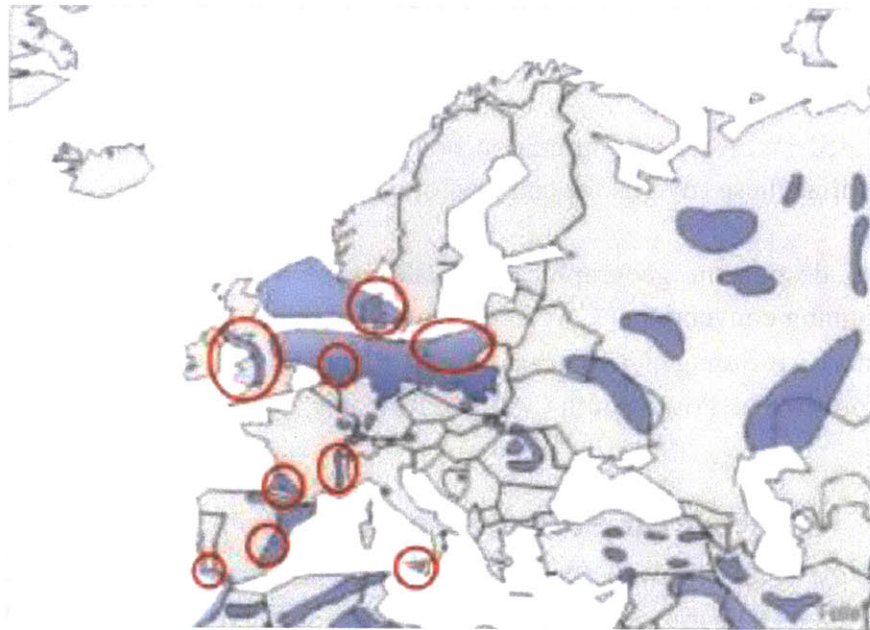
Figure 6 Superimposed image of high wind resources map and geologically available regions for CAES installations in Europe [14]

Northern Germany, Belgium, Western UK, Eastern Coast of Spain, southern part of France and Sicily/Italy are places where high wind potential overlaps with underground salt caverns. It is also stimulating for ORES deployment in the Mediterranean, namely Spain, France and Italy, where wind profile is decent, demand is high and depths are promising.
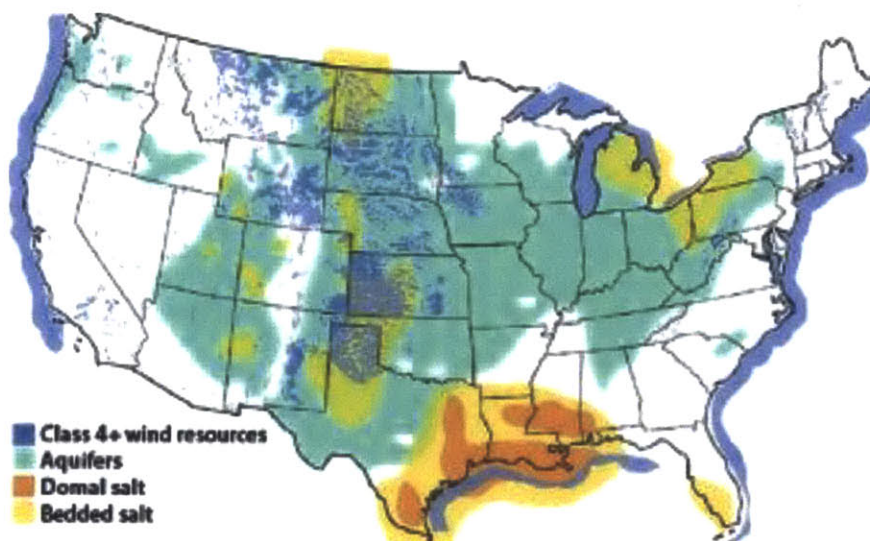
Figure 7 Superimpose of high wind resources with geologically available regions for CAES installations in US [14]

Similarly southern part of US; Texas, Louisiana, Mississippi and Alabama are available for CAES installations. Furthermore corresponding offshore wind speeds in the region are encouraging for FWTs. There is intensive energy consumption in these states due to high temperatures in the summer and heavy usage of air conditioning. Because of this high energy usage, concentrated highly on late afternoon hours, energy price makes peak which creates an opportunity to utilize these caverns for energy storage.

However, despite the geographical availability of regions in Europe and US there are currently two running conventional CAES plants in the world:
- Huntorf Air Storage Gas Turbine Power Plant, in Huntorf, Germany
- McIntosh- The PowerSouth CAES in Alabama, United States

2.1.2.1.   Huntorf Air Storage Gas Turbine Power Plant

In 1978, the Huntorf Power Plant (HPP) was commissioned in lower Saxony, Germany, an area known for its salt mines. The HPP is designed to serve peak load and competes with natural gas fired power plants. The main difference between HPP and traditional gas turbine power plants is that the generation of electricity and compressed air do not happen at the same time at HPP. This facility pumps air at off-peak times into two salt caverns, which lie in depths of 800 and 650 m and have a total volume of 310,000 m^3. The plant was initially built with a nameplate capacity of 290MW; capacity was later increased to 321MW. During high demand, compressed air is released and burned with NG and then used in a gas turbine to generate electricity. The gas turbine used in the facility is capable of immediate start (without a long ramp-up time) and can reach the full output of 321MW within six minutes." [15]. Figure 8 below is a schematic of the facility.
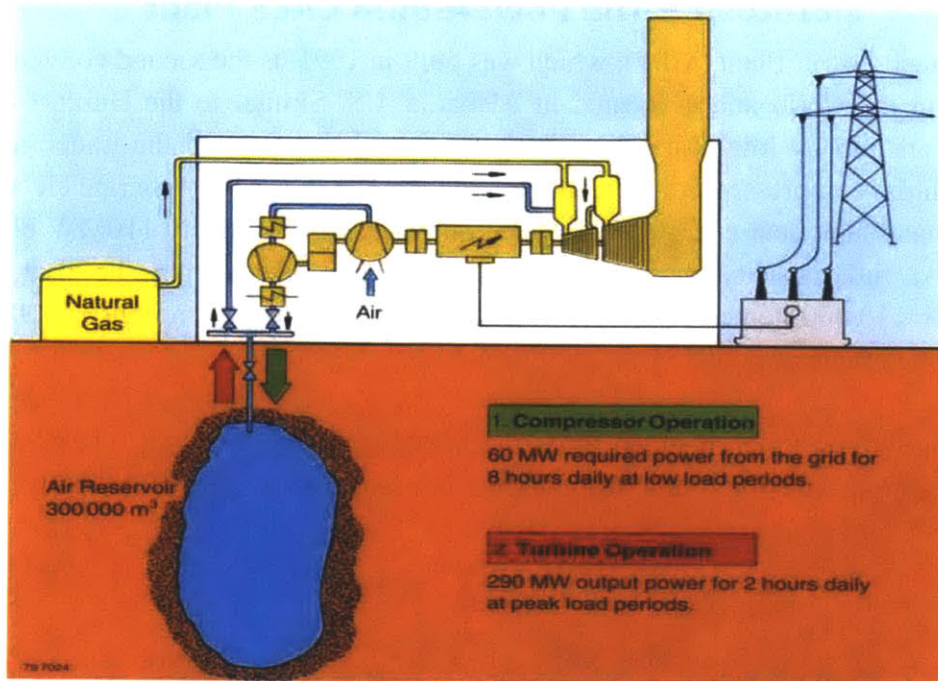
Figure 8 Schematic of Huntorf Air Storage Gas Turbine Power Plant[1]

      The publically available system parameters for the Huntorf plant are summarized in Table 4 below [16].

Table 4 Specifications of Huntorf Power Plant

Turbine Operation	321 MW (for less than 3 hours)
	Air flow rate: 417 kg/s
Compressor Operation	60 MW (for less than 12 hours)
	Air flow rate: 108 kg/s
Caverns	Number of Caverns: 2
	Cavern 1 Volume: 140,000 m³
	Cavern 2 Volume: 170,000 m³
	Minimum pressure: 1 bar
	Minimum operational (exceptional) pressure: 20 bar
	Minimum operational (regular) pressure:43 bar
	Maximum permissible & operational pressure: 70 bar

---

[1] Huntorf plant was renovated. As a result of this, reservoir volume was increased to 310,000m³ and power output was upgraded to 321MW. However no updated schematic related to plant's current status is published in company's website or public materials

2.1.2.2. McIntosh – The PowerSouth CAES Plant

McIntosh Power Plant (MPP), which was built in 1991, is the second conventional CAES power plant in the world and is located in Alabama, US. Similar to the Huntorf Power Plant, compressors are run by low-cost energy at low-demand times to fill the underground storage reservoir with the compressed air. The compressed air is then used to generate electricity during the peak-demand/high cost energy times. MPP output is approximately 110MW electricity (for 26 hours). At full capacity the power plant is capable of meeting the peak demand of approximately 110,000 homes [17]. McIntosh CAES plant can serve roughly 3000 average US homes for a one month period [18].

During the peak/high demand times the MPP can reach its output, 110MW of electrical power, in a ramp-up time of 14 minutes. Figure 9 is a schematic of the MPP facility.
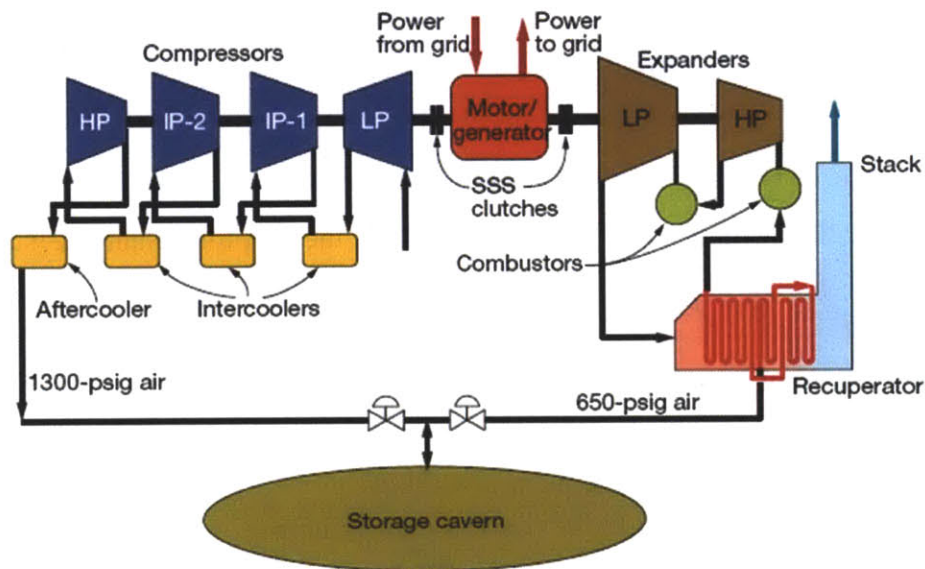
Figure 9 Schematic of McIntosh Power Plant

To store energy air is drawn through Low Pressure (LP) compressors and then compressed through 4 stages (LP, Intermediate Pressure (IP)-1, IP-2 and High Pressure (HP) compressors). During compression energy from grid is used to run the compressors. Between each stage compressed air is cooled via intercoolers. High pressured air after the last (4th) stage runs through an aftercooler before it is stored in the caverns to maximize cavern storage capacity.

When power is needed, compressed air is released from the caverns and preheated by the recuperator. Pre-heated air is then combusted by NG and runs the first set of HP turbines. Exhaust of HP turbines is burned again before it runs the LP turbines. Relatively high

temperature exhaust of LP turbine, compared to cavern temperature, is used in the recuperator to preheat the inlet of the HP turbines and then released to the atmosphere.

2.1.3.   Thermal Mass CAES

The process is often called *adiabatic CAES*, however for the purpose of this paper it will be referred to <u>thermal mass</u> since heat is transferred to and from the system during the processes of compression and expansion. Thermal mass CAES is an innovative method of CAES, with a thermal mass as an additional unit operation. In a thermal mass CAES system, the thermal energy generated as a result of compression is stored in a thermal mass, which is either liquid or solid selected for its heat transfer and retention capacities, so that heat is reused during expansion. Such a system offers numerous advantages over traditional CAES, reducing temperature in the storage tank, reduces heat loss through the tank walls, increasing the tank energy storage capacity, and reduces the rate of oxidations.

To charge the system, electricity is drawn from the grid to supply a motor which in turn drives a compressor. As the air is compressed, it rapidly generates heat. To later utilize this heat, the hot air passes through a heat exchange mechanism. Several concepts have been proposed for the heat exchange mechanism including: (1) the use of a conventional heat exchanger to transfer heat between the air and a thermal storage medium such as oil, and (2) a self-contained drum with heating tiles to absorb, retain and transfer heat as the hot air passes through. The thermal medium, whether heating tiles or oil, retains the transferred heat for later use and the cooled air is stored in a pressure vessel or natural salt cavern. ESPC, a US based power consulting firm, has discussed a design similar to that described in option 1 above, while RWE, a European-based company, is currently working on the ADELE project utilizing the heat transfer mechanism described in option 2 [19] [20].

To discharge the system, the compressed air in storage is drawn into use again. Because the expansion results in a substantially lower air temperature (which in turn could affect the integrity of the turbine) the air passes back through a heat exchange mechanism for thermal interaction with the thermal storage medium to regain heat prior to entering the expansion process. After the heat exchanger the air undergoes expansion through a power generation device such as a turbine which in turn drives electricity back to the grid. A process flow diagram (PFD) for the Thermal Mass CAES system as described is shown in Figure 10.
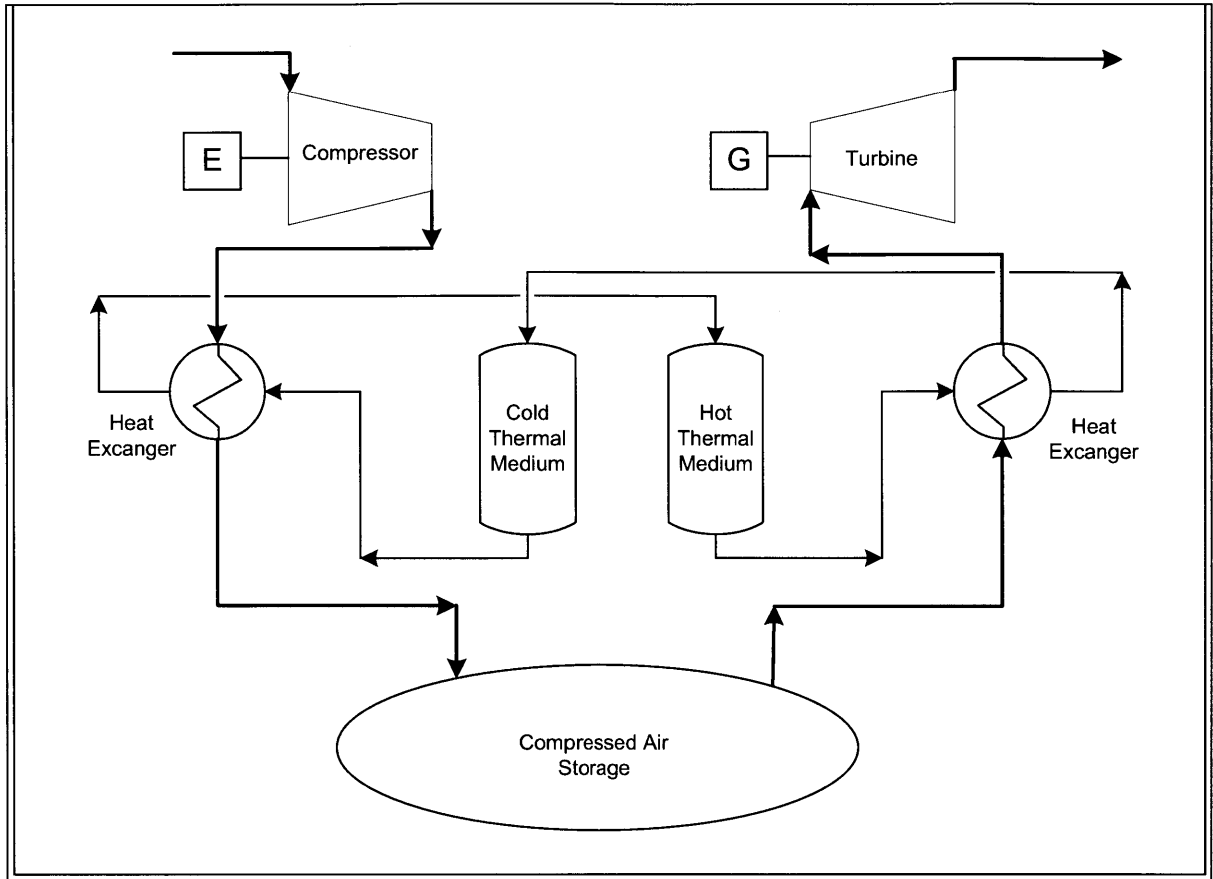
Figure 10 Process Flow Diagram (PFD) of Thermal mass CAES

The publically available system parameters for the ADELE plant, a thermal mass CAES plant, are summarized in Table 5 below [20].

Table 5 Specifications of ADELE CAES Plant

Compressor	Max pressure at outlet: 100 bar
	Max temperature at outlet: 600 Celsius
Thermal Mass	Height: 40 m
	Material: bed of stones or ceramic molded bricks
Cavern	Max pressure: 70 bar
Turbine	Max power: 300 MW
	Max duration per cycle: 3.3 hours
Overall	Round trip efficiency: 70%
	Energy stored: 1000 MWh

2.1.4. Innovative PSH or CAES Applications

Hydrostor, a Toronto based company, is seeking for innovative ways to store energy underwater [21]. The company aims storing compressed air in underwater flexible bags which are anchored at the bottom to overcome buoyancy forces. Hydrostatic pressure of water column is used to keep the bags pressured. Similar to thermal mass CAES to store energy compressed air runs through thermal energy storage to transfer excess heat to the storage tank and when energy is needed relatively cold compressed air due to the lower temperatures of sea water runs back through the same thermal mass, heats up and runs a turbine [22]. The capacity of the system is limited to the depth of the bags, thermal energy storage capacity of the thermal mass and heat transfer rate (a function of material properties and contact surfaces). A schematic of Underwater Compressed Air Electrical Storage (UCAES) is shown in Figure 11.
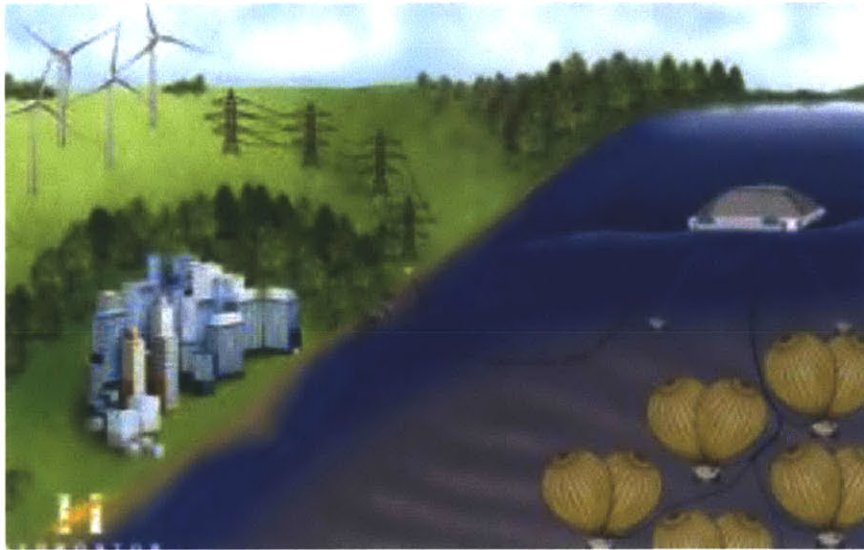
Figure 11 Underwater Compressed Air Electrical Storage – Hydrostor (source:[22])

Two German physicists Horst Schmidt-Böcking and Gerhard Luther worked on a similar concept to the ORES to store energy underwater in spheres [23]. The idea is similar, build hollow concrete spheres which are envisioned to have 280m diameter, deploy them under water in depths of 2000m, and use them as a lower reservoir. When energy is needed high pressure water will run into the sphere through a turbine and generate electricity. Water is pumped through the same reversible turbine (i.e. Francis turbine) to charge the spheres. They envision storing 58,000MWh in their device. A schematic of their research is shown below in Figure 12.
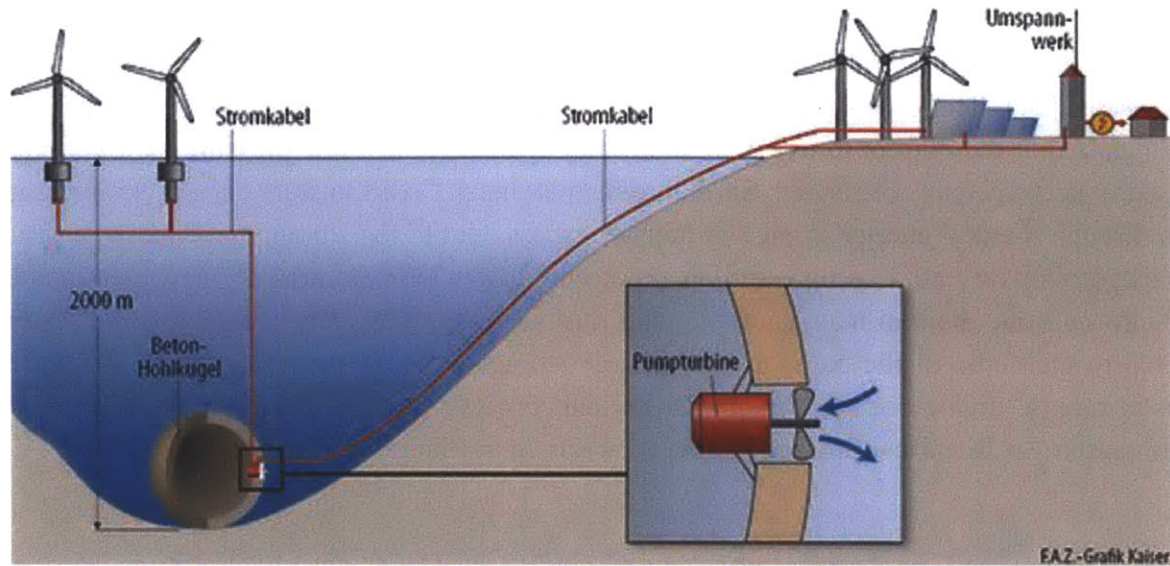
Figure 12 Schmidt-Böcking & Luther's hollow sphere energy storage device (source:[23])

In addition to prior implementations a UK professor from Nottingham University, Seamus Garvey, envisions building a hydraulic ram using low pressure high flow rate tidal power to generate high pressure and low flow rate and storing 25 megajoules of energy per cubic meter [24].

Chp 3. ORES

3.1. Early Stages and Operating Concept of ORES

ORES units are hollow concrete structures which can store utility scale energy and provide anchorage for offshore energy harvesting platforms. ORES concept was first created by Prof. Alexander H. Slocum as a conical energy storage platform co-located with offshore energy harvesters, most notably, offshore wind, current and tidal. ORES can facilitate great integration of renewable energy at higher levels of penetration. First design of ORES concept is presented in Figure 13 as a conical, hollow, concrete structure on which energy harvesting devices can be mounted.
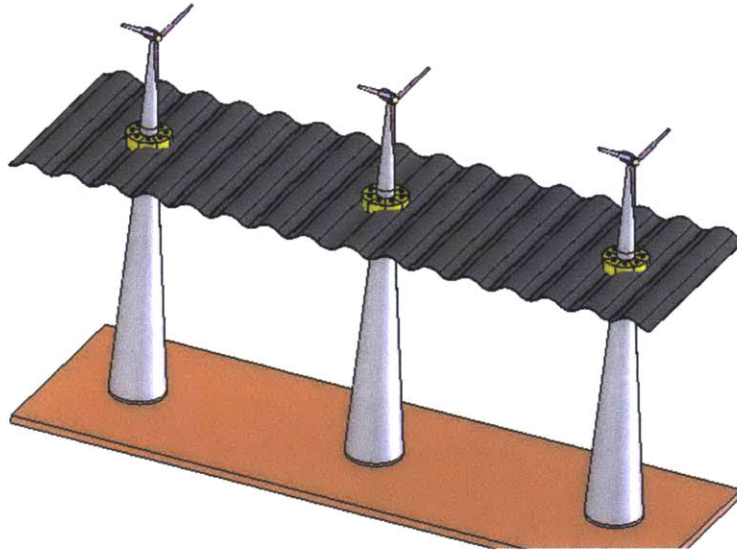
Figure 13 Initial conical energy storage platform co-located with offshore energy harvesters by Prof. Alexander Slocum

These ground mounted conical structures didn't allow installations for far offshore energy harvesters. Alison Greenlee then joined the project in 2008 and worked on subsea chambers which replaced conical structures [25]. She designed and analyzed chambers with hexagonal prism and cylinder with a spherical end cap. Instead of mounted conical platforms these chambers, connected to each other and filled with rock, could provide sufficient anchorage for mooring floating platforms so that even greater depths and farther areas from shore could be exploited for better winds.

After 2009, extensive research on both economics and design was conducted by Gregory Fennell [26]. During this period, spherical ORES design evolved and was evaluated. Hexagonal and cylindrical geometries were revised and studies focused on spherical structures [27]. These structures were designed to function as a lower reservoir for PSH. Energy is stored during the

off-peak times or when there is excess renewable energy by pumping water out of the sphere. When there is a demand on the grid or energy prices are high, water is allowed to run into the spheres under hydrostatic pressure of water through a turbine and electricity is generated. ORES project evolution since 2007 and operating concept can be seen in Figure 14 and Figure 15 respectively.
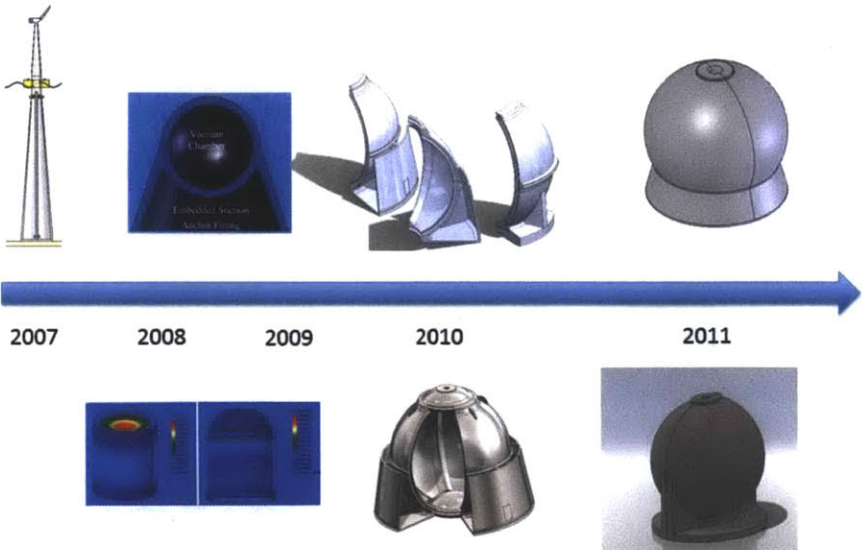
Figure 14 Evolution of ORES project
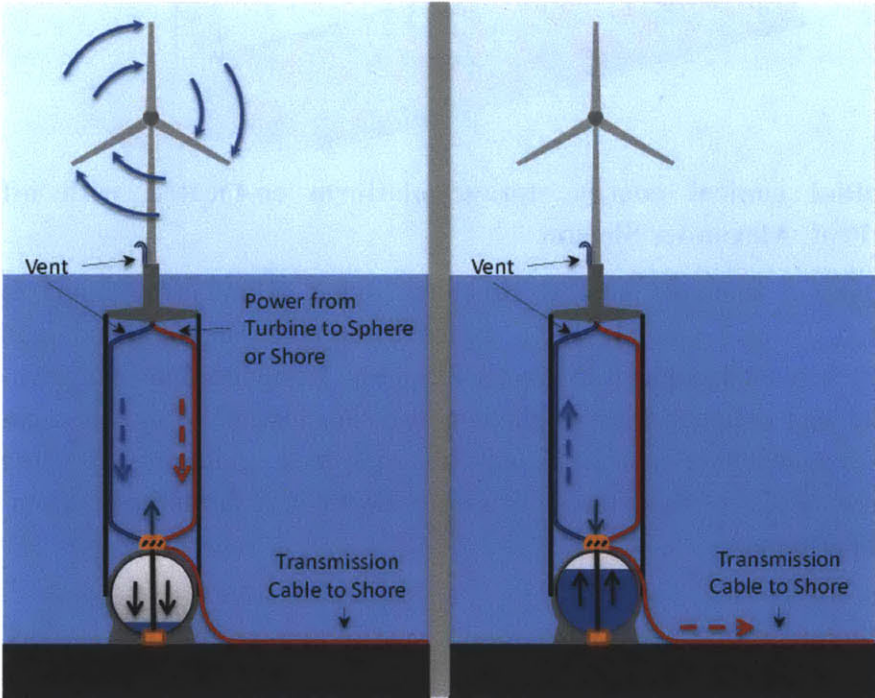
Figure 15 ORES operating concept acting as anchorage for Tension Leg Platform

As mentioned earlier ORES spheres act as the lower reservoir of a PSH system and hydrostatic pressure is the governing force to store energy. The energy capacity of the system can be calculated as:

$$E[MWh] = \frac{\rho_{sw} \times g \times h \times V_{sphere} \times \eta_{pump} \times \eta_{turbine}}{3600000000} \qquad (2)$$

Conventional PSH typically works with round trip efficiencies of 70-85% [28]. To be conservative side of the calculations 70% round trip efficiency and 95% of volume utilization is assumed. Volume utilization refers to the ratio of actual volume of the water running into the sphere to the inner volume of the sphere. 5% accounts for the volume of sphere which cannot be used for reasons including the minimum head for the pump to operate and not make cavitation and air pocket which remains when sphere is full with water. Resulting ORES capacity as a function of depth and radius is shown in Figure 16.
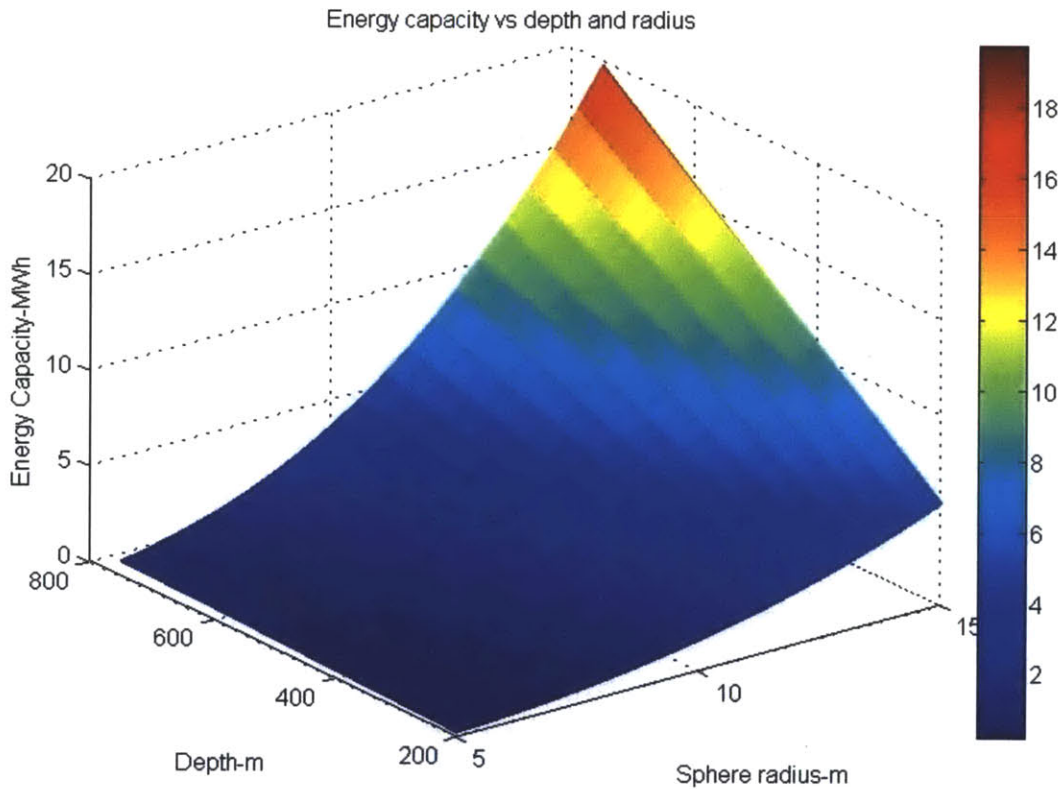
Figure 16 ORES energy capacity as a function of depth and diameter

Figure 16 clearly illustrates that greater depths and larger radius favor the capacity of each ORES sphere and the system as a whole. However despite being technically feasible it is not economically feasible to work at deeper depths than 800-900m. High costs associated with special equipment and advanced Unmanned Autonomous Vehicles (UAVs) make it challenging to deploy spheres and maintain rotating equipment at 900m depth.

35

3.2. *Innovating for Manufacturability*

Manufacturing ORES spheres is neither an easy nor an impossible process. There are two main challenges awaiting the full-scale mass production. First is the high production rate. In order to build 1GWh storage field at 750m depth consisting of 27m inner diameter (ID) ORES spheres in one year, 70 spheres should be manufactured, towed, deployed and connected to the grid. This production rate yield a sphere fully connected to the grid in 6 days. In order to achieve this goal complicated design features should be eliminated without compromising the structural strength. Steel rebars are avoided and replaced with increased wall thickness to overcome high hydrostatic pressures. Increased wall thickness allows excess ballast to act as sufficient anchorage for TLPs and catenary mooring for FWTs. ORES spheres acting as catenary mooring is shown in Figure 17.
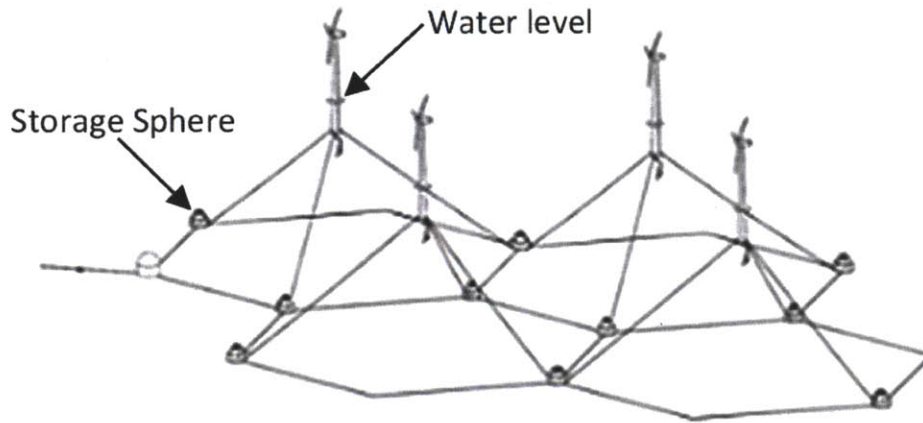
Figure 17 ORES spheres used as catenary mooring for FWTs [27]

500mt ballast for catenary mooring and 3000mt ballast for TLP are required for FWTs [29]. Minimum wall thickness at equilibrium state for buoyancy is calculated as:

$$W_{sphere} = F_{buoyancy} \tag{3}$$

$$\rho_{concrete} \times g \times \frac{4}{3} \times \pi \times ((r+t)^3 - r^3) = \frac{4}{3} \times \pi \times (r+t)^3 \times \rho_{sw}$$

When equation (3) is solved with values for an equilibrium state, wall thickness is derived as 10.8% of diameter.

An additional conical base is required to act as a cradle and hold the sphere. The conical base envisioned and calculated in [26] is revised to facilitate manufacturing. The new approach is sketched in Figure 18.

36
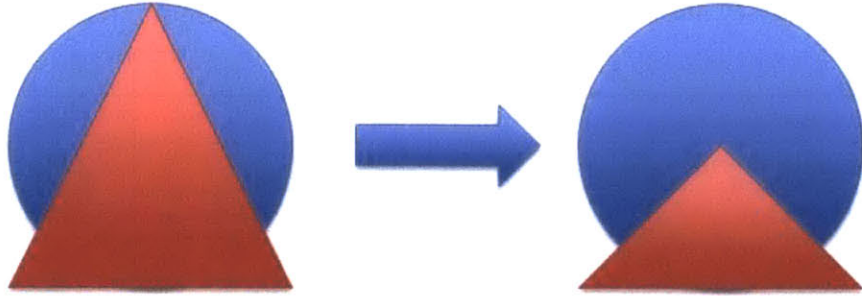
Figure 18 Revision of conical cradle for ORES sphere [26]. (Previous design on the left, updated design on the right)

This revision provides a more realistic calculation while avoiding double-counting of the wall intersecting at the bottom of the sphere. Volume of conical base is calculated as:

$$V_{Conical\_Base} = \frac{1}{3} \times \pi \times h \times r^2 - \int_0^R \left(\int_0^\phi 2 \times \pi \times r^2 \times \sin \phi \, d\phi \right) dr \qquad (4)$$

All this data and equations (3) and (4) are incorporated into an Excel spreadsheet and data including volume, capacity, mass, ballast, volume of concrete for each sphere is calculated in Table 6.

Table 6 Storage capacity and volume calculations of ORES (an updated study of [30])

Density sea water (kg/m^3)	**1025**	
Density concrete (kg/m^3)	**2400**	
Inside diameter (m)	**27**	
Concrete strength (MPa, psi)	**34.5**	**5000**
Strength Factor of Safety	**1.5**	
Minimum ballast safety factor	**1**	
Inner volume (m^3)	**10306**	
Required ballast for total inner volume (mt)	**10564**	
Volume - conical base: height=base D=sphere D$_{inside}$ (m^3) (Eq. 4)	**1443**	
FWT anchor system	**Moored**	**TLP**
Required ballast for anchoring FWT (mt)	**500**	**3000**
Total required submerged ballast (mt)	**11064**	**13564**
Volume of concrete required for ballast (m^3)	**8046**	**9864**
Approximate sphere wall thickness to self-ballast (m)	**2.9**	**3.8**
Actual submerged weight of concrete (mt)	**13141**	**17576**
Actual dry land weight (mt)	**22937**	**30678**
Actual ballast safety factor	**1.2**	**1.3**
Pump/turbine efficiency	**70%**	**70%**
Percent useable volume (to maintain pump head height)	**95%**	**95%**
Planned deployment depth (m)	**400**	**400**
Charge capacity at 400m (MWh) (Eq. 1)	**7.6**	**7.6**
Maximum safe depth (m)	**671**	**799**
Charge capacity at maximum safe depth (MWh)	**12.8**	**15.3**

Table 6 indicates that dead weight of 27m ID ORES sphere with a 2.9m wall thickness and a conical base is 22,937mt. Moving a monolithic structure with a 32.8m OD and weighing 22,937mt easily on manufacturing plant is not a trivial process. Ship industry is using low bed heavy duty trucks to carry and move ship segments which can weigh hundreds of tons. Bridge construction is another industry which deals with the same problem. Big size bridge segments are constructed at the manufacturing facility and moved with low bed truck and loaded on heavy duty trucks or trains for longer distance transportation. Examples of heavy segments in different industries being carried by low bed trucks are shown in Figure 19.

Figure 19 Examples of low bed heavy duty trailers carrying ship segments (on the left) and bridge/tunnel segments (on the right) (source:ttnet.net)

Another method used heavily in shipyards is rails. Big segments are built on site and transferred/carried to next stage or another place via rail network. Even though carriage capacity of rail system is substantially higher than it is for low bed trucks, building the infrastructure for a rail network is costly and the modifications of the network is highly restricted. Regardless of the methodology securing and safely moving spherical concrete structures will be time and skill intensive. In order to overcome this challenge some new approaches and design were developed. Some of these improvements and alternative approaches will be discussed in the following section.

3.3. *Vertical Hemispheres*

This concept was first developed with Prof. Alexander Slocum, Gregory Fennell and Gökhan Dündar [26]. Each hemisphere is envisioned to be poured vertically. The idea was developed to overcome the complex assembly procedure of multiple-stave design. This approach will eliminate the requirement of high capacity cranes to lift horizontal hemispheres. Furthermore having vertical hemispheres instead of multiple-sliced staves will allow match-casting to enhance sealing in the contact surfaces. In the multiple-sliced design all of the parts should be assembled simultaneously otherwise final assembly cannot be accomplished. Comparison of multiple-stave design with vertical hemisphere design is shown in Figure 20.

Figure 20 Multiple-stave sphere (on the left) compared to hemisphere design (on the right) (credit Alex Slocum)

Compared to complex geometry of 6-stave design, vertical hemisphere design is simpler and eliminates multiple alignment issues. A closer look of the male-female joints of the bottom part of the staves and contact surfaces can be seen in Figure 21.
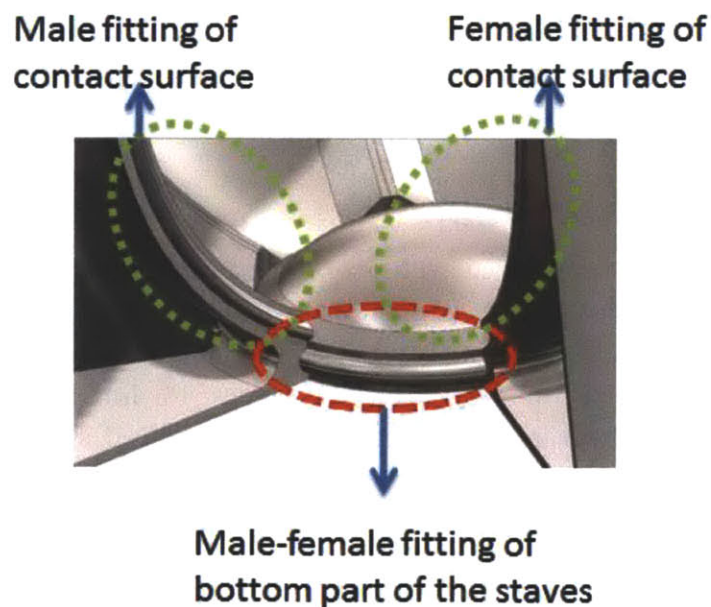
Figure 21 Male-female fitting of bottom part and contact surfaces of staves

Even though male-female fitting on the bottom parts of the staves provides sealing and a better alignment, additional match-cast features on the mating surfaces (male and female fitting of contact surface) make it impossible to assembly unless all pieces are assembled simultaneously.

Main production concept for the vertical hemisphere design is having an inner and outer mold. Molds are attached to each other via flanges. After molds are assembled concrete is poured to the space in between from the port at the top of the mold. There are three key characteristics of the design:

- Match-cast surface to enhance sealing of the mating surfaces
- A surface at the back of the hemisphere where rotating equipment can easily and precisely be mounted
- Conical base to provide sufficient anchorage for catenary mooring or TLP for FWTs.
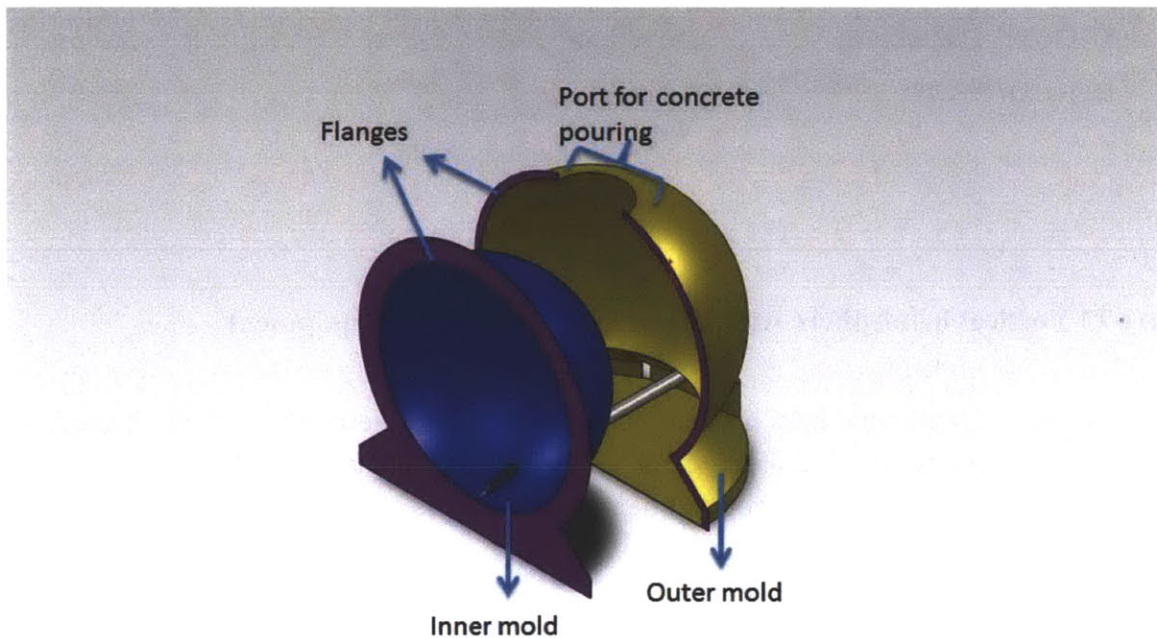
Figure 22 Exploded view of mold assembly describing key features

However some features are added to or taken from the initial design with to meet the arising or changing requirements. Rotating equipment installation has been subject to numerous design iterations and was studied intensively. Initially an extruded boss parallel to the ground at the back of the hemisphere was developed. The idea here is to provide surface to install pump/turbine unit on top of this boss and connecting to a pipe that directly goes into the sphere. This approach can be seen in Figure 23.
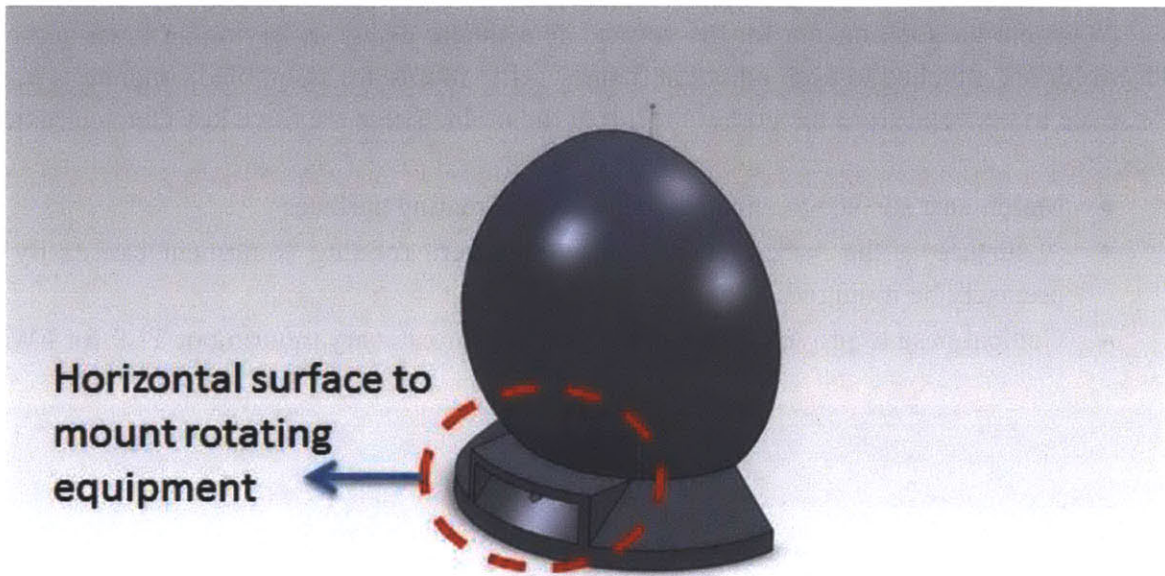
Figure 23 Vertical hemisphere with a boss to mount rotating equipment

Building a horizontal boss makes it hard to demold the hemisphere. A draft angle should be applied in order to provide a smoother demolding. This improvement was applied to the design and inclined boss feature replaced the horizontal boss. This approach is shown in Figure 24.
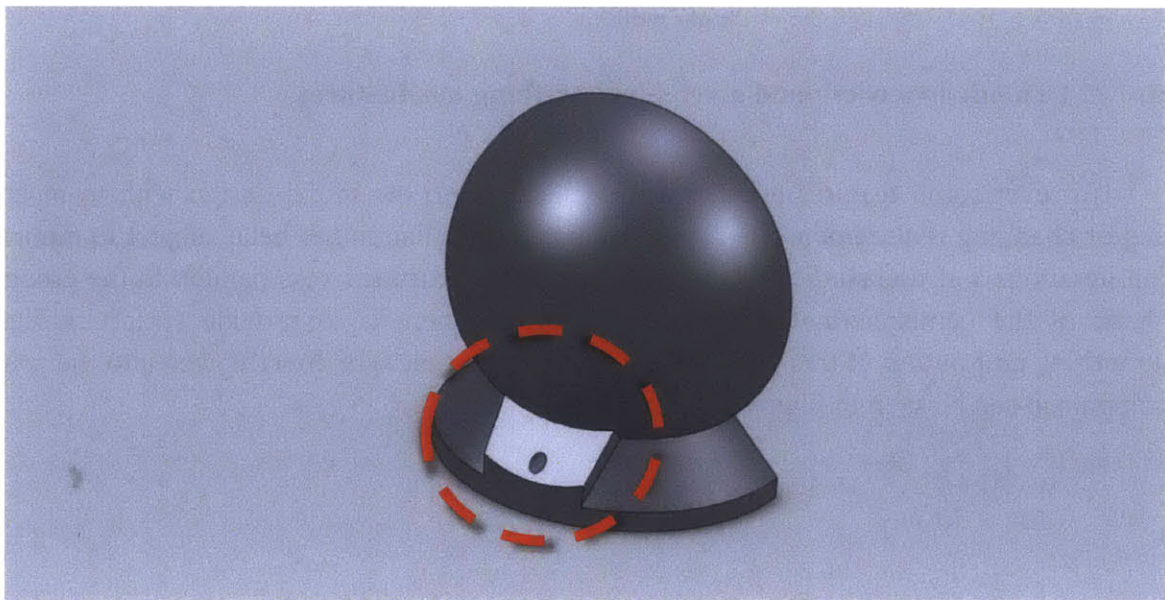
Figure 24 Vertical hemisphere with inclined boss and 5^0 draft angle to mitigate demolding problems

It can be seen in Figure 24 that the boss is revised and designed as inclined surface. In addition to making the boss inclined a 5^0 draft angle is introduced on the both sides of the boss. Despite the fact that designing an inclined boss with draft angle mitigates demolding problems it is still a complicated feature for full-scale ORES sphere. Mounting the pump/turbine unit precisely on this inclined boss is not simple either. Precision of the installation and complexity of the structure led us to create an innovative approach, *plug-and-play*.

Rotating equipment can be lowered by using tension legs as guideline and can be plugged to its place. A male probe at the bottom of the pump/turbine unit will fit to its female probe on the sphere side. When plugged in male probe will automatically open the valve on the female side so that it can start operating. When plugged out the valve will close automatically and prevent water running into the sphere. This plug-and-play capability has been used in the Navy for replenishment at sea (RAS) operation and will increase the operation efficiency of the system by eliminating the long maintenance and installation procedures. A schematic of RAS showing male and female probe is shown in Figure 25.
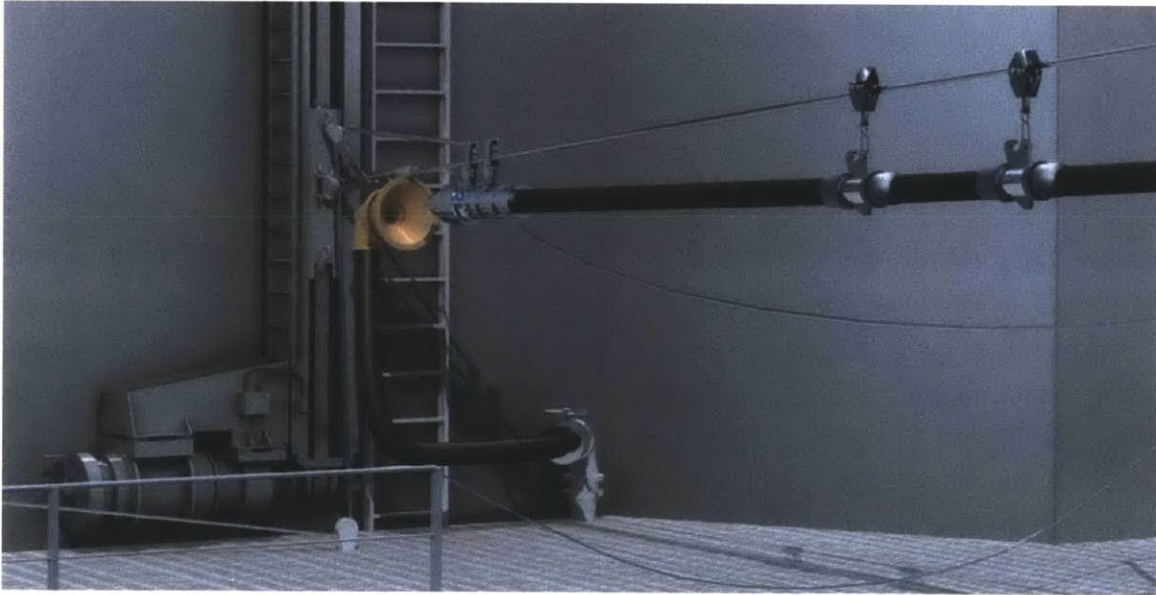
Figure 25 Schematic of RAS showing male-female joint (source: http://www.rolls-royce.com/marine/products/deck_machinery/dm_naval/ras/)

3.4. Inner Balloon Method

Vertical pouring added value to the project in terms of manufacturing. It is easier to pour concrete, to move the hemisphere around the manufacturing site and requires less specialized and heavy duty equipment compared to horizontal hemisphere approach. To make the manufacturing process even easier some innovative ideas were generated yet none of them could be experimented because of the time constraints.

First solution is using a rubber balloon as inner mold. Similar to the vertical pouring there is going to be two vertical molds, assembled to form a spherical outer mold. A polyurethane or rubber balloon is going to be placed in the mold. Concrete is going to be poured simultaneously while a same density fluid is pumped into the balloon. Balloon will be attached to the bottom and various points to the pouter mold to overcome buoyancy forces and maintain concentricity. In order to test this model rubber 22cm diameter volleyball is used as inner balloon and 24cm hard plastic bowl was used as outer mold. After the third trial a perfect sphere with uniform wall thickness was achieved. Figure 26 shows the experiment and the final sphere cast from plaster.
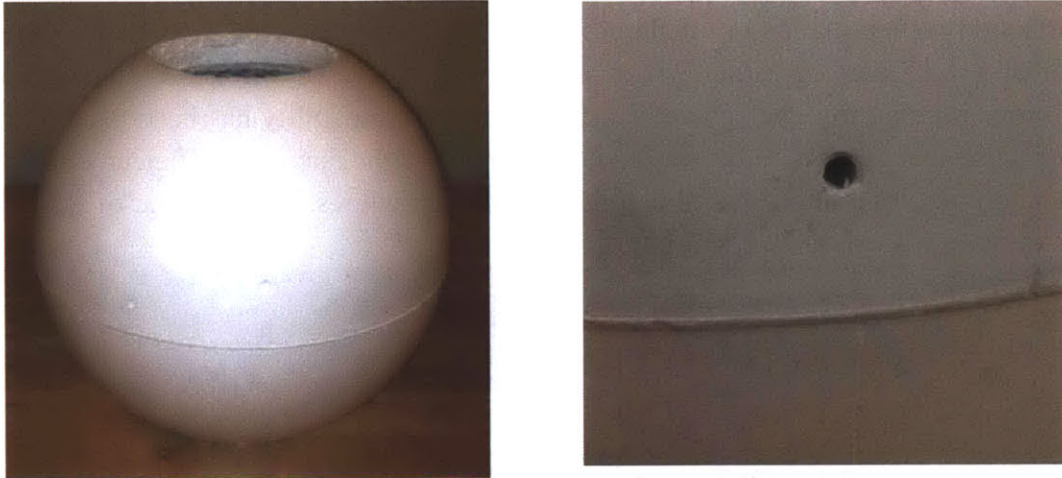
Figure 26 22cm ID plaster sphere using inner balloon method. Threads for maintaining the concentricity is shown on the right picture (credit: James Meredith)

Initially water was decided to be used to fill the balloon. The advantage of water is abundance, low price and ability to be easily to transported (pump and discharge). Density of water is 1000kg/m^3 compared to 2400kg/m^3 of self-consolidating concrete. The difference between the densities results in less hydrostatic pressure of water compared to the hydrostatic pressure of the same column of wet concrete. In addition to pressure differential problem low density results in less weight of the balloon when totally filled with water thus more force to be compensated to attach the balloon to the mold. Buoyancy force applied to the balloon totally submerged to the wet concrete can be calculated as:

$$F_{buoyancy} = V_{submerged} \times \rho_{concrete} \times g \tag{5}$$

$$F_{buoyancy} = \frac{4}{3} \times \pi \times 12.5^3 \times 2400 \times 9.81 = 192.6E6 \ [N]$$

It can be seen that buoyancy force applied to a fully submerged balloon is very high (192000 kN) hence large displacements and deformations are expected in the balloon. The SW simulation of rubber balloon, filled with water and fully submerged in the wet concrete is shown

in Figure 27. It can be seen that if rubber ball is not properly pressurized and contacted to the mold hydrostatic pressure of wet concrete will squeeze the balloon upwards and will result in total deformation of balloon.
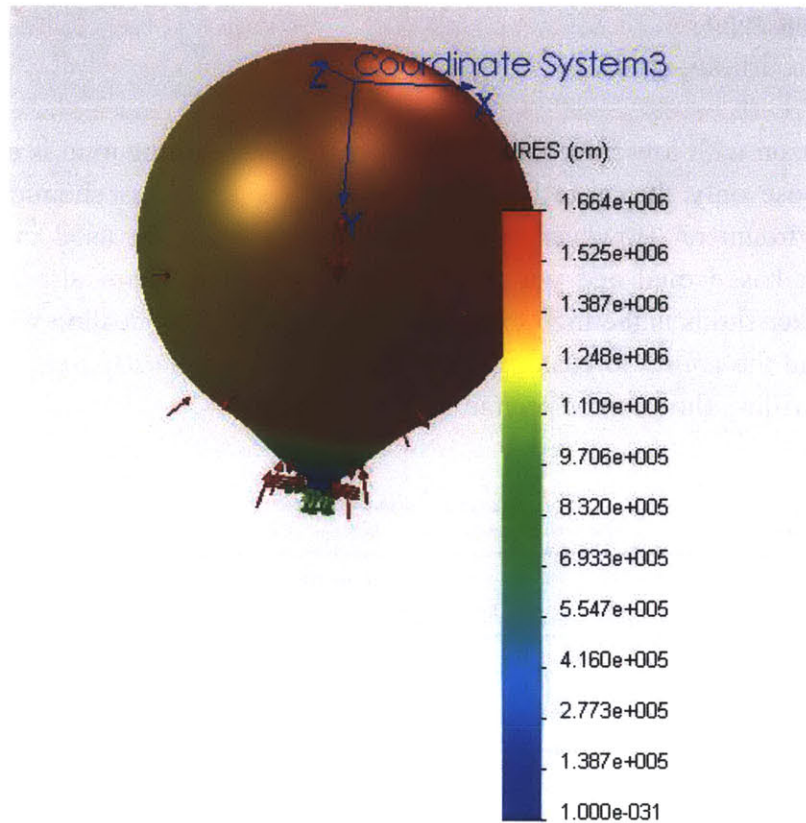
Figure 27 Displacement of rubber balloon filled with water and fully submerged into wet concrete

However because of the pour rate and cure time the balloon will never be totally submerged in wet concrete. If an average $100m^3/h$ concrete pour rate [31] and 2 hour for initial curing time is assumed for the concrete to carry its own weight, this yields approximately 4cm of wet concrete volume (depending on bottom, medium or top part of the sphere. 4cm example is from the medium part of the sphere). Low pour rates will have a negative impact on the total pour time but will decrease the buoyant and contact forces applied to mold and the balloon. Based on our experience and tests done in American Concrete, Maine, concrete starts to cure immediately after the mix and can carry its own weight after one hour. To be on the conservative side two hours is assumed for the concrete top carry its own weight. Our tests, results and experience gained related to the concrete are going to be discussed in Chp 5 with more detail.

Drilling fluid was also evaluated to replace water. Drilling fluid, known as drilling mud, is a fluid comprised of different elements including water, clay, barite etc., to maintain the

borehole stability, avoid it to collapse, clean the drill bits and remove drill cuts during drilling process. There are three types of drilling fluid [32]:

- Water based mud
- Oil based mud
- Gaseous drilling mud

In comparison with low price and abundance of water, drilling mud is expensive and can be found on purpose only. It has to be treated carefully since it has chemicals which can be hazardous for environment. However drilling mud envisioned to be used in ORES project is going to be water based mud and will not have high abrasive chemicals. The superiority of drilling mud to other fluids is the high expertise of drilling industry dealing with different kinds of drilling mud and the ability to customize the density to meet the requirements of the project. Various types of drilling fluid can be seen in Figure 28.
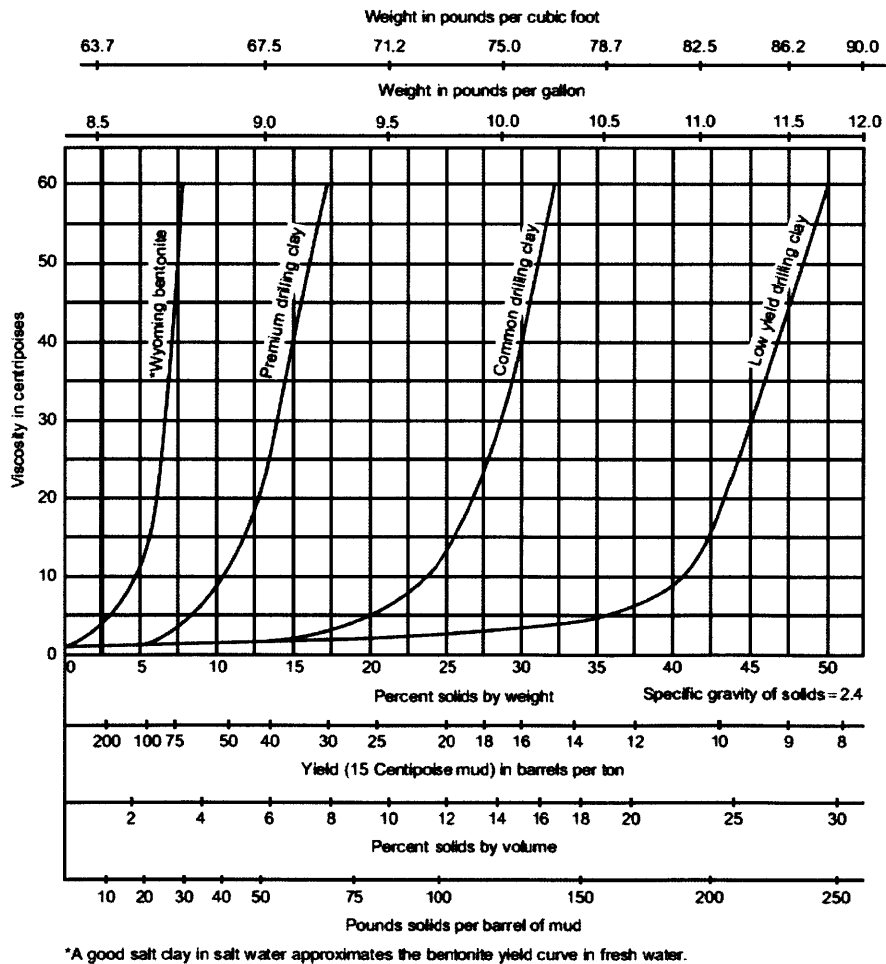
Figure 28 Types of drilling fluids and corresponding densities with respect to composition (source :(The University of Texas at Austin - Petroleum Extension Service, 1969))

46

Common drilling fluid density changes between 1200-1400 kg/m³. However density of the drilling fluid can be increased by increasing the barite content in the mud. Density of barite is approximately 4200kg/m³ [33]. It is not assumed pollutant by most of the countries hence widely used to adjust the density of the drilling fluid when deeper holes are dug and to be maintained.

3.5. Consumable Steel Mold

We wanted to assess the feasibility of marginal approaches after conventional methods. Mold for multiple uses would be expensive and should be replaced after some use. Furthermore, molds would require maintenance which can affect and even halt the manufacturing process. We, ORES team, wanted to calculate the cost of disposable steel molds which can eventually replace multiple use high-cost molds.

HY60 steel was selected because of its wide range of applications in various industries. Volume of the steel was calculated by using thin shell approximation. During the calculations steel thickness was calculated to withstand the maximum hydrostatic pressure of concrete during the pour. To be conservative with the calculations it is assumed that full sphere is filled with wet concrete thus maximum pressure is calculated as:

$$P_{max} = \rho_{concrete} \times g \times D \tag{6}$$

$$t = \frac{r.P_{max}}{2\sigma} \tag{7}$$

The volume of the mold is calculated with thin shell approximation as:

$$V_{mold} = 4 \times \pi \times r^2 \times t \tag{8}$$

Approximate cost for processed stainless steel is assumed as $4,000/mt [34]. All of the assumptions and equations (6), (7) and (8) are incorporated to an Excel spreadsheet and cost estimations are calculated. Table 7 shows the result of disposable steel mold.

47

Table 7 Volume and cost estimates of disposable steel mold

		as % of inside diameter	UNITS
Sphere Wall Thickness	11%		
Allowance for Ribbing/Connections	25%	as % of mold steel	
ρ_concrete	2400		kg/m^3
σ_HY60 Steel	2.76E+08		Pa
ρ_steel	7.9		mt/m^3
Cost of Steel [34]	$4,000		$/mt
	Inner Mold	Outer Mold	
Diameter	27	32.94	m
Hydrostatic Pressure	635688	775539	Pa
Mold Steel Thickness	0.01555	0.02315	m
Surface Area	2,290.2	3,408.8	m^2
Steel Volume	35.6	78.9	m^3
Extra Steel for Ribbing/Connections	8.9	19.7	m^3
Sub-Total (volume)	44.5	98.6	m^3
Sub-Total (mass)	351.7	779.2	mt
Sub-Total (cost)	$ 1,406,927	$ 3,116,813	
Total Cost of Steel	$ 4,523,740		

Inner and outer disposable molds that can resist the hydrostatic pressure of the wet concrete cost $1.4M and $3.1M respectively and a total sum of $4.5M. In addition to the material cost, there will be additional labor cost, deployment cost, pump/turbine unit cost and cabling costs as well as contingencies which will make disposable mold option economically not feasible.

Another challenge with the approach is the corrosion. HY-60 is not corrosion resistant thus oxidation will start immediately with the deployment. After some period small particles from corroding parts will break. These parts will be sucked in during the charging process and could damage the turbine blades as they go through the pump/turbine unit. One solution to the corrosion could be Cathodic Protection (CP). CP refers to an anti-corrosion measure widely used on ships and marine industry which converts the *valuable metal* (the metal that is protected) to the cathode of an electrochemical cell. This method requires a sacrificial anode to be attached to the surface of the valuable metal so that it erodes instead of the surface. One downside of the technology is that the sacrificial metals should be renewed in time because they are consumed

(sacrificed) to protect the metal. In addition to the periodic replacement they should also be monitored continuously since not all of the anodes work perfectly due to the quality of the connection between the surfaces. Another disadvantage of the CP is the fact that it enhances marine growth on the surfaces. Application of CP results in more marine growth which increases the likelihood of ingestion. Another solution can be covering the surfaces with antifouling paint. This paint will help to suppress the marine growth however it should be renewed with time too. Since the ORES structures cannot be moved back to surface for maintenance this solution is not sustainable either.

3.6. Shotcrete use in ORES

In addition to vertical hemisphere and disposable mold method the feasibility and cost of shotcrete to build ORES spheres should be evaluated. Shotcrete is a method to spray concrete through a nozzle with pressurized air. Since it is not a new material or composition but a method of application it has the same material properties with the concrete, 34.5MPa compressive strength in 28 days and 2,400kg/m^3 density [35]. It has been used since 1900s mainly to repair/patch structures. Recently shotcrete has been started to be used in construction industry, particularly in constructing spherical buildings.

The concept of using shotcrete in building hemispheres or sphere is simple. It requires one form, either inner or outer mold. To promote manufacturing using an outer mold seems more applicable and enables a fully automation. When a full spherical mold is assembled an automatic controlled nozzle is inserted into the mold. A sketch of shotcrete implemented to ORES outer mold is shown in Figure 29.
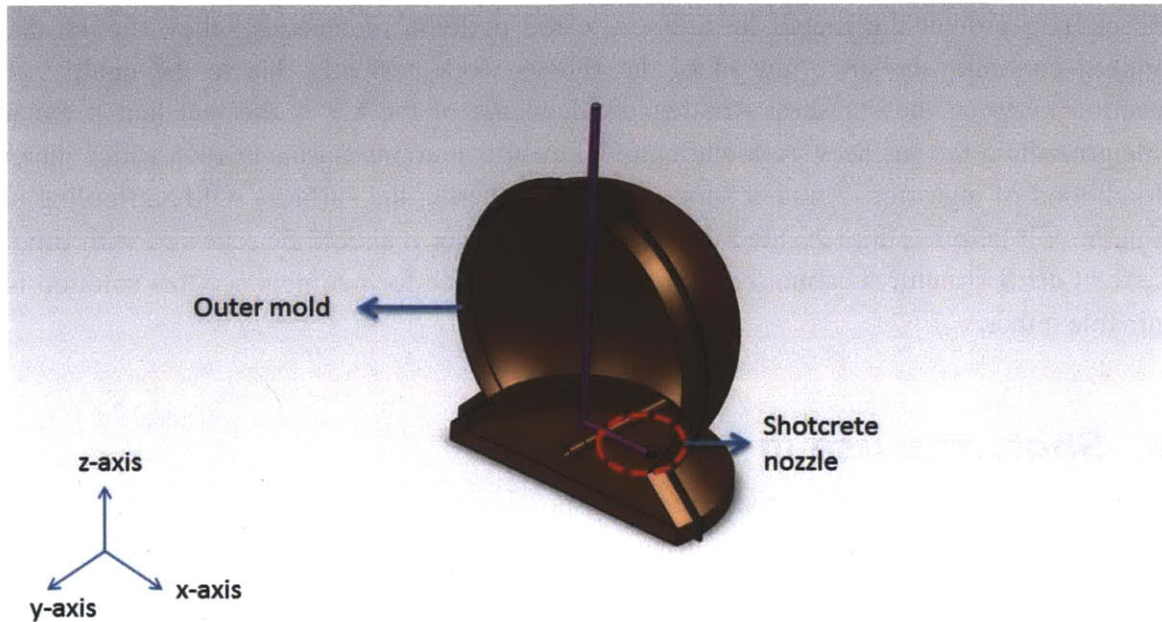
Figure 29 Cross section of ORES shotcrete concept

After nozzle assembly is secured to its position and aligned with the mold it will start rotating and spraying concrete to the inner walls of mold. Shotcrete nozzle assembly needs to have 3 degrees of freedom; rotation around z-axis, transformation along z-axis and transformation along y-axis. Three degrees of freedom can be precisely and easily be maintained and controlled. Similar to 3D printing walls are going to be poured by layers on top of each other eventually forming the required thickness. 914mm wall thickness has been achieved with single layer and greater wall thicknesses can be achieved. Shotcrete can be poured with 10-20m^3/h rate [35]. Slow pour rate compared to conventional pouring will increase the pour time on the other hand it will start curing in the process of manufacturing which can decrease cure time. Due to the lack of sufficient data about the applications further study should be conducted in detail before applying to ORES project. An automated shotcrete and an example of a shotcrete dome are shown is Figure 30.

Figure 30 Automatically executed shotcrete (on the left Source: http://www.multicretesystems.com/shotcrete) and shotcrete dome (on the right source: http://www.reedpumps.com/concretedomes.htm)

Despite being technically feasible applying shotcrete also has some challenges. The biggest issue is the excess heat of hydration for wall thicknesses greater than 1m. Curing process is an exothermic reaction which generates heat and this heat is called "*heat of hydration*". ORES spheres are envisioned and designed to be bigger in diameter than 27m with 2.9m wall thickness. In such an application greater wall thickness will generate more heat during curing process and have less heat transfer through convection thus resulting in increasing temperature of the concrete. If heat of hydration is not removed properly it will form micro-cracks in the structure resulting in loss of structural strength. One solution to this problem is prefabricating steel cages that cooling pipes can be attached to and using the steel cage as reinforcement. However this method will also increase the complexity of the project. One innovative solution to steel rebar is having a spiral cage. Depending on the size of the sphere and required structural strength a spiral steel reinforcement can be laid clockwise and counter-clockwise so that they intersect in various points to enhance strength. Solid Works (SW) model of spiral cage steel reinforcement is shown in Figure 31.
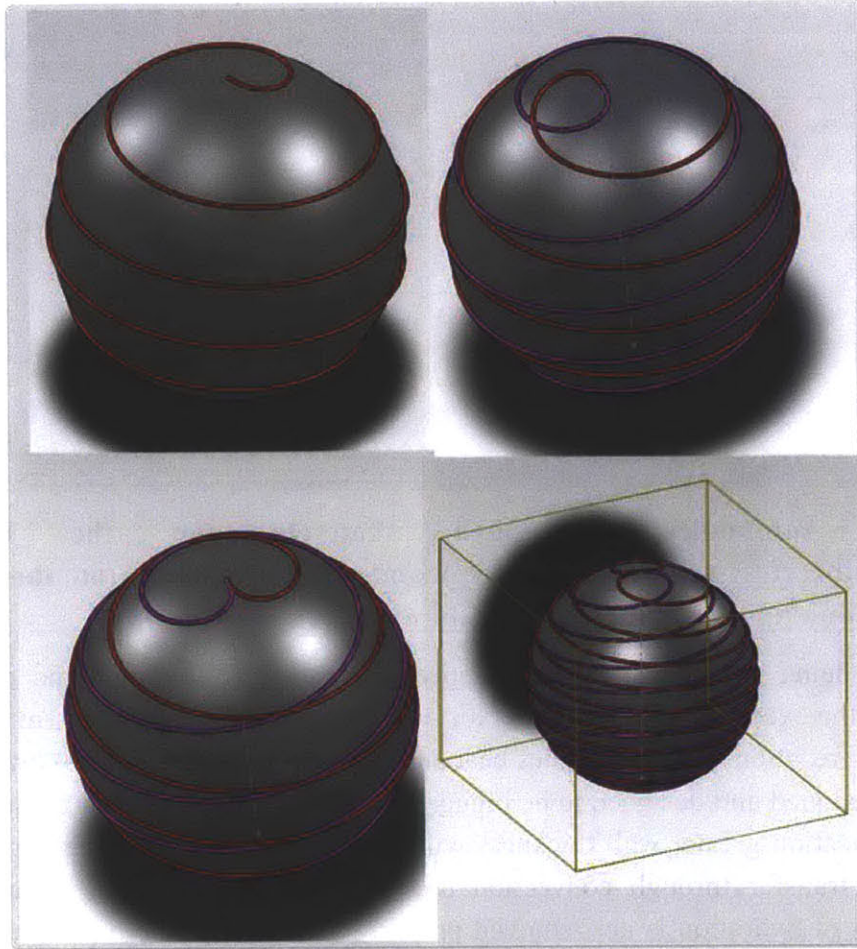
Figure 31 Spiral cage steel reinforcement and cooling system

Besides heating problem shotcrete also requires special equipment and highly skilled labor. These requirements make manufacturing process slow and expensive. Nevertheless, building large storage fields requires a dedicated facility. If shotcrete is going to be the main manufacturing means labor cost and equipment cost will substantially decrease over the duration of the project.

3.7. Bottom Hemisphere and Rings

In all of the scenarios described so far the common problems are manufacturing a monolithic single pour sphere, moving the sphere from one station to another during the manufacturing process and lack of vessels and equipment to deploy 20,000mt sphere. Before simulating other geometries we wanted to finally evaluate a sphere comprised of rings. Match-cast pipes and cylindrical segments with various sizes that can reach up to 20m ID and 100m in length is widely used in tunnel constructions [36], aqueducts, irrigation channels, water distribution network and sewage systems.

ORES rings idea is building the bottom part as a hemisphere and building the remaining sphere out of concrete rings. Hemisphere is going to be poured and will cure while top rings are poured separately. Each segment is going to be match-cast relatively positioned with the previous ring. Therefore misalignment between the match-cast parts will be eliminated.
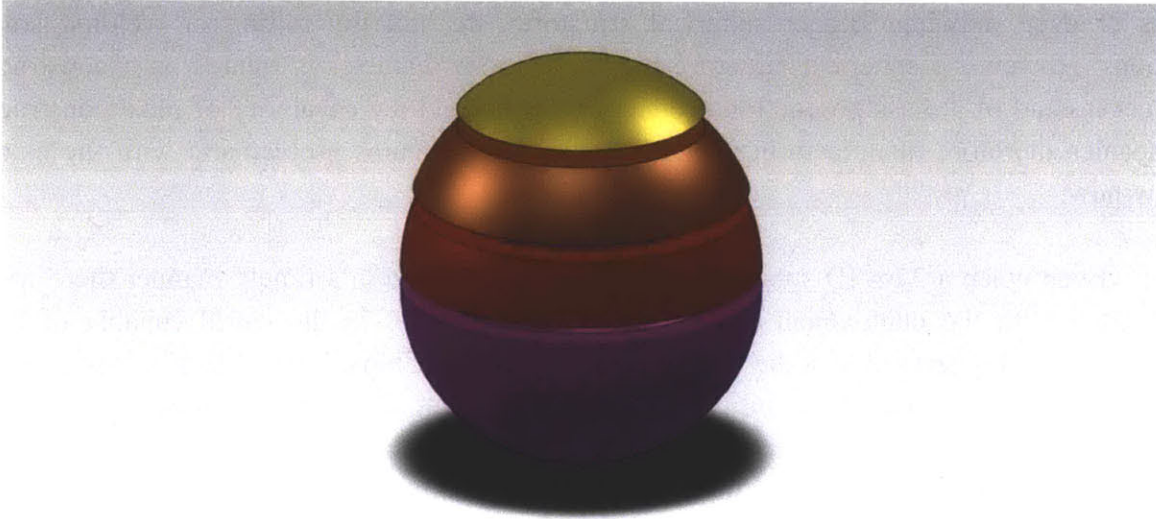
Figure 32 Solid model of ORES sphere comprised of rings

Thickness and the number if the rings should be calculated for each individual scenario to optimize manufacturing process and reduce labor costs.

Advantage of this method is the ability to carry and deploy each ring individually and more easily. Multiple slices can be loaded to the vessel to be used for deployment and can be handled more easily due to the smaller weight and size of each ring compared to the whole weight of the spheres. In addition to their distributed weight gravitational center of the total load will be lower compared to the vertical hemispheres which will have a positive effect on the stability of the vessel.

Chp 4.   Alternative Geometry

Sphere design has a structural advantage to overcome the hydrostatic pressures compared to other geometries; however large spheres have mass production and deployment issues. Steel spherical heads with smaller dimensions (less than 1m diameter) are manufactured either by press or deep drawing. Bigger spherical structures are built by rolling or welding smaller sections. However a spherical structure bigger than 3m diameter is treated as a construction project instead of a mass production product and is beyond the capability of most construction companies therefore manufacturing spherical structures remains problematic with the existing know-how.

Even when a 27m ID spherical structure is constructed in a timely manner there will be challenges with the deployment. There are not many cranes in the world capable of lifting 20,000mt. The biggest crane in the world, Taisun located in China, is capable of lifting 20,000mt [37]. Because of the limited capability of existing equipment, deployment can be achieved either by loading the structures onto a vessel or by using barges to sink the spheres in a controlled manner and leverage the buoyancy force. Loading the spheres onto a vessel can be accomplished by using a rail system. Depth of the ports should be deep enough for the vessel to take water into its ballast tanks to semi-submerge to enable the transfer from dock to the vessel. MV Blue Marlin a semi-submersible heavy lift ship which carried USS Cole after a terrorist attack in Yemen, is shown in Figure 33. It requires 30m depth to load its maximum capacity cargo. Because of the fact that there are not any ports in the world which has a 30m depth, cargo is towed to open sea and then loaded to the ship. However this is not the best option for ORES. First it requires an additional transportation vessel/barge to tow the spheres and load it on the ship. In this case the same barge can be used to transport the sphere to the deployment site. Second transportation from dock to the barge remains still problematic.

Figure 33 MV Blue marlin carrying USS Cole after a terrorist attack in Yemen

Our studies show that even though manufacturing 27m ID spheres is challenging but technically feasible, deployment of the spheres is also challenging with the current design. In order to solve mass production and deployment problem we evaluated the feasibility of horizontal cylinders.

4.1. Capacity Calculations

Tubes have been widely used for different purposes including water transportation, sewage, tunnels etc., and it is a well-established industry. As a consequence of being widely used in many industries a great experience has been gained hence industry can meet different demands and production rate of pipes is significantly high. James Meredith has calculated the difference in safe deployment depth of thin wall assumption versus thick wall assumption in his master thesis [38].
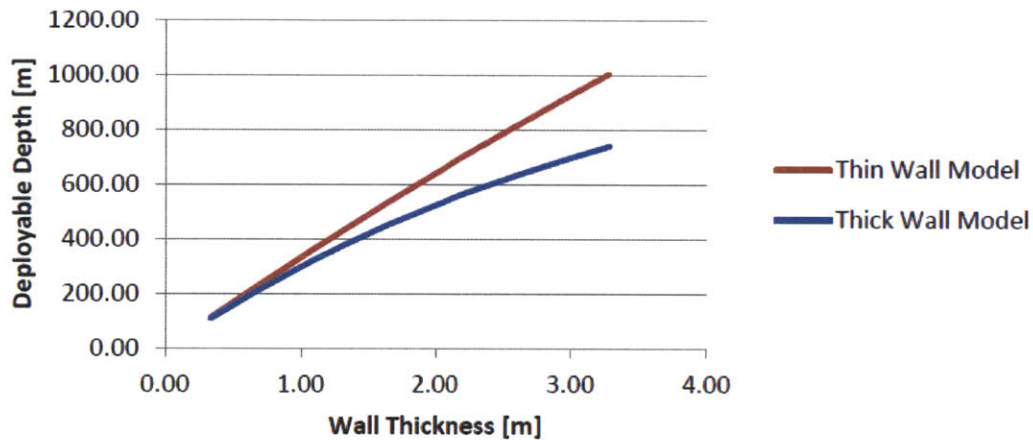
Figure 34 Maximum deployment depth as a function of wall thickness according to both thin-wall and thick-wall assumptions

James concluded that thick wall assumption is required and yields to shallower depths compared to the same wall thickness with thin wall assumption. According to the calculations, thick wall assumption should be used to determine the wall thickness and safe operating depth. All the assumptions are incorporated into an Excel spreadsheet and results are shown in Table 8.

Table 8 Underwater energy storage cylinder stress and capacity calculations under thick-wall assumption (credit: Alexander H. Slocum)

Material	Concrete	Steel	Sphere
Internal Pressure, Pi (N/mm^2, psi)	0.00		
Water Depth, Po (N/m^2, meters H2O)	2000000	200	
OD, Do (m)	23.40	18.056	
Wall thickness/ID	15%	0.2%	12%
ID, Di (m)	18	18	27.0
wall thickness, t (m)	2.700	0.028	3.2
length (depth into page), L (m)	45.72	45.72	
Interior volume (m^3)	14688.0	14687.95	10306.0
exterior volume (m^3)	26370.8	14789	19649.7
Structure density (kg/m^3)	2400	7900	2400.0
seawater density (kg/m^3)	1025	1025	1025.0
Structure mass (tonne)	28039	798.6	22424.8
pump/turbine efficiency	70%	70%	70%
Charge capacity (MWh)	5.7377	5.7377	4.0
energy/structure mass (kWh/tonne)	0.205	7.184	0.180
displaced seawater (tonne)	27030	15159	20141
net ballast (tonne)	1009	-14360	2284
Ballast safety factor (must be greater than 1)	1.04	0.05	1.11
Ballast	It stays on bottom	Add Ballast!	It stays on bottom
Overall size of wind farm (MW)	5	5	5
Hours of storage desired	12	12	12
Amount of storage required (MWh)	60	60	60
Number of cylinders required	10	10	15
Total weight of all cylinders (tonnes)	293,208	8,351	234,500
Material strength (MPa)	50	500	50
safety factor	1.5	1.3	1.5
design stress	33.3	384.6	33.3
stress ratio (hydrostatic stress/max design stress)	0.25	1.45	0.00
	STRESS OK	CAUTION STRESS TOO HIGH	

Chp 5.   3m Zorb Ball Concrete Pouring Experiments

5.1. Introduction and Purpose

After manufacturing the 90cm ID concrete sphere and testing it onshore for proof of concept, we started designing the second step in ORES project, 3m ID prototype. Building and assembling 3m prototype will provide us valuable information about choosing the proper equipment for pipe fittings, how to make the pipe connections to mitigate externalities that can cause pouring interruptions, creating checklists to standardize manufacturing process and adjusting the internal pressure to avoid collapse of the wet concrete wall.

Constructing domes or building other forms of spherical structures from concrete is neither a new idea nor a new engineering capability. However, manufacturing ORES spheres is envisioned as a mass production to boost US manufacturing competitiveness and create more green jobs. It will also enhance the implementation of renewable energy portfolio standards (RPS) while providing storage for intermittent renewable energy resources. In order to achieve this goal a new approach should be utilized to increase the manufacturing capacity of the existing concrete plants. We came up with the conclusion of using a Zorb ball, a toy for grown-ups with two concentric spheres with 3D spokes connecting the spheres while maintaining an air cushion in between, for inner and outer mold [39]. The Zorb ball being used for our experiments is shown in Figure 35.

Figure 35 Zorb ball (3.6m OD, 3m ID) being tested in Lobby 7, MIT

Zorb ball is made of polyester based Thermoplastic polyurethane (TPU). Some physical properties of TPU are stated as [40]:

- Superior abrasion resistance for high wear applications
- Elevated tensile strength for durability
- Good memory retention
- High resistance to hydrocarbons, chemicals, ozone, bacteria, fungus
- Waterproof
- Easily fabricated using thermal bounding, laminating, die cutting or vacuum forming
- Flame retardant.

Its superiority in physical properties was decisive for choosing TPU ball instead of PVC ball.

5.2. The Hypothesis

In our field trip to American Concrete, MN, we wanted to test and observe behavior and the compressive strength and behavior of the early stage concrete slump. Initial experiments on wet concrete provided insights and valuable experience for pouring and manufacturability of the 3m ID concrete ball which will eventually be applied to full-scale ORES spheres.

5.3. Materials and Methods

5.3.1. Design Study

90cm ID prototype was envisioned as two horizontal hemispheres made from concrete poured between two pressure vessel heads. Having two hemispheres resulted in some difficulties while mating and sealing the contact surfaces. Experience gained from the manufacture of the first prototype motivated us to have innovative approach for manufacturing the 3m ID prototype.

Methods for building the 3m ORES prototype are listed as:
- Inner and outer vertical hemisphere mold made from steel
- Disposable steel sphere mold
- Steel outer mold and inner balloon
- Inner and outer balloon mold

At first glance using a steel mold looks like it is superior to its alternatives. Steel mold without a proper cooling system will face some challenges. During the curing process water reacts with concrete thus generates heat which causes the steel molds to expand. Concrete must stay still while curing and the expansion of the mold will induce micro-cracks in the concrete resulting in a distortion in the micro integrity of the concrete hence reduction in the structural strength.

58

The equation to calculate the expansion of the steel is stated as:

$$\frac{\Delta A}{A_0} = 2 \times \alpha \times \Delta T \tag{9}$$

where ΔA is the area differential resulted by the temperature difference, α is the thermal coefficient of the material and ΔT is the temperature difference. Temperature increase and heat generation in the early stage wet concrete can be seen in Figure 36 [41].
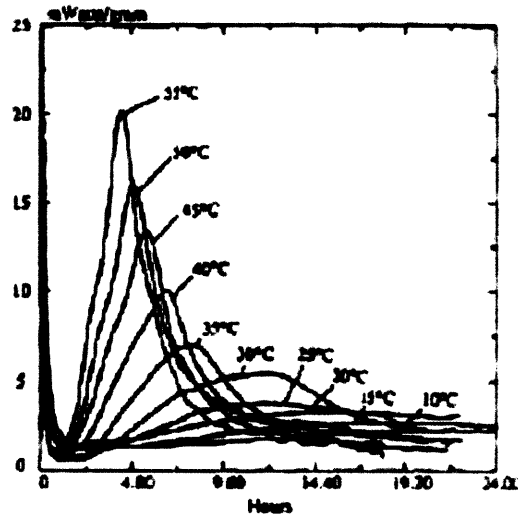
Figure 36 Heat of hydration: Type I cement (Copyright ASTM International) [41]

Area differential resulted by the temperature differentiation is calculated by combining (1) with the data from Figure 36:

$$\frac{\Delta A}{4 \times \pi \times 1.8^2} = 2 \times 1.22E^{-5} \times (328 - 291)$$

ΔA is calculated as 0.035764 m². Calculating the expanded radius accounting for the expanded area results in:

$$4 \times \pi \times r_{new}^2 = 4 \times \pi \times 1.8^2 + 0.035764$$

From the Equation (9) r_{new} is calculated as 1.80079. It can be concluded that there is a 0.79 mm increase in the radius yielding a 0.04% displacement. The increase in the radius is insignificant compared to 1.8m radius. The results of the calculation prove the potential in using steel as a mold in smaller scale. However full-scale molding will require additional cooling to mitigate the effects of heat of hydration.

59

Deformation of mold during curing process causes cracks in the concrete which results in decrease in the strength. Effects of deformation were tested and cracks on the surface of curing concrete can were observed with bare eye shown in Figure 37.

Figure 37 Cracks due to changing mold geometry

5.3.2.   Preparations

Building a concrete hollow sphere using Zorb ball has some challenges. In order to eliminate all the externalities which can interfere the pouring, intensive amount of research and study has been conducted. In order to pour concrete monolithically with minimal disturbance on the concrete surface 3x3inches pipe fittings with gate valves were attached in every 1m height. A sketch of the pipe positions on the ball is shown in Figure 38.
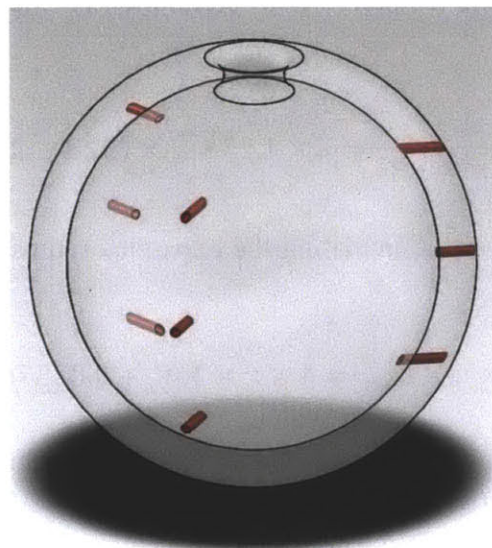
Figure 38 SW model of Zorb ball with pipe installations

3 inches pipe fittings with gate valves on each are attached to the outer shell of the ball with 120^0 and the joints were then sealed to prevent air leakage. Bill of Materials (BOM) will be given in the appendix.

5.3.3. Pouring Methodology

Concrete is mixed at the plant and put into $1m^3$ buckets. A sub-hopper which acts as a funnel is hung at the bottom of the bucket. A flexible pipe, names as elephant trunk to pump fluid concrete is attached at the end of the sub-hopper. A lever on the bucket is used to allow the concrete flow to the sub-hopper then through the elephant trunk to the ports attached. After pouring required amount of concrete, gate valve is closed and pipe is attached to the next port.

In order to avoid the Zorb ball to slump, ball will be encircled with 1m high plates which will be filled simultaneously with the ball to provide a cradle for the ball. In addition to having a cradle for further support of the ball both inner sphere (3m ID) and the air cushion between the balls will be kept under pressure during the pouring process. SW model of concrete ball resting on its cradle after curing is shown in Figure 39.

Figure 39 SW of Zorb ball resting on the cradle/base

Upper part of the Zorb ball will be closed with a reinforced wooden gate on which an eyeball and pipe fittings for pressure instrumentations are attached. SW model of reinforced wooden gate is shown in Figure 40 next to the real manufactured plywood gate. The gate was initially tested for 0.5psi.
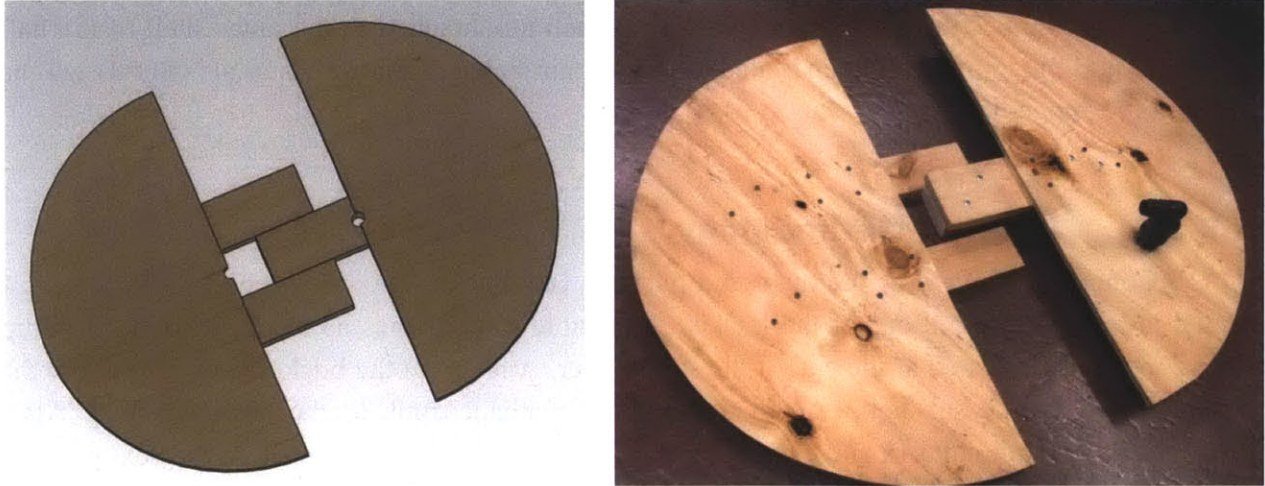
Figure 40 Wooden reinforced gate (on the left SW model, real gate on the right)

FEA of wooden gate is shown in Figure 41. It can be seen that 1st principal stress of the gate under 3.5 psi pressure is 4.5 MPa, far below yield stress of wooden gate, 20 MPa, and maximum displacement is 0.79mm. Under these conditions Factor of Safety (FOS) of the simulation is 3.34. After initial FEA, the gate was tested up to 1 psi and no plastic deformation observed. However gate should be tested with 4psi for the sake of the project.
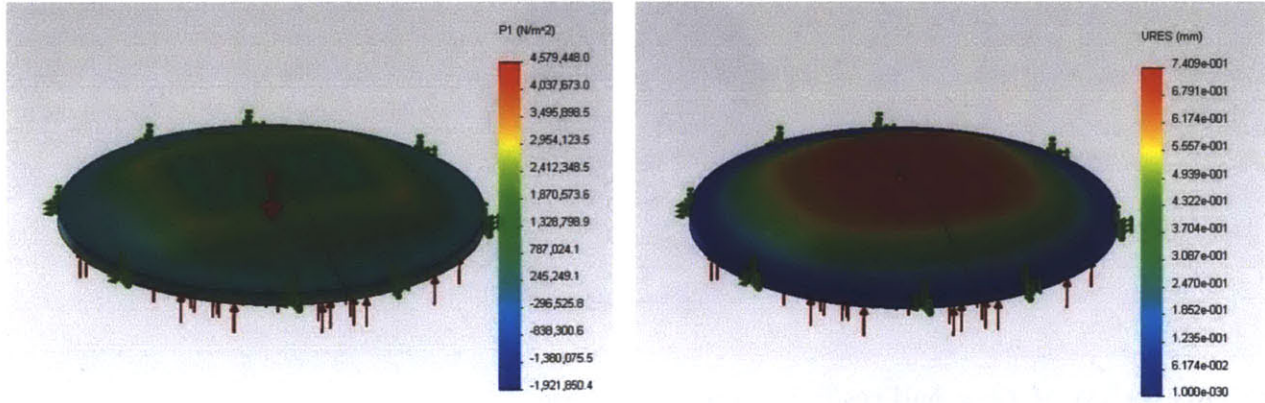
Figure 41 1st Principal stress and displacement of wooden gate under 3.5 psi

The manhole at the top will be enclosed by the wooden gate and then both inner sphere and the air cushion, where concrete will be poured, will be pressurized with blowers. Both blowers will be mounted on the ground and 2.54cm ID plastic pipe is going to be used to connect the blowers with the blower ports on the Zorb. Pressure drop through the pipe is calculated by Hagen's equation as [42]:

$$\Delta P \approx 0.316 \times \left(\frac{\mu}{\rho V D}\right)^{1/4} \frac{L}{D} \frac{V^2}{2g} \tag{10}$$

When L=6 [m], ρ=1.275 [kg/m^3], μ=1.9E-5 [Pas], d= 2.54E-2 [m], V=16.9 [m/s] is applied the pressure drop through the pipe is calculated as 83.4Pa which is insignificant. Assuming internal sphere will be less than 3.5psi (23.8kPa) corresponding concrete height can be calculated as:

$$23786 = \rho_{concrete} \times g \times h$$

If we apply ρ=2300 kg/m^3, g=9.81m/s^2 concrete column height is calculated as 1.05 m. However in order to be conservative not more than 20cm concrete column will be poured and pouring will be subject to field experimentation according to the physical behavior or Zorb ball. Since exact material properties for Zorb ball and strings, used as 3D spokes, couldn't be obtained from the manufacturer an exact FEA for the Zorb ball with 3D spokes under hydrostatic pressure of concrete and internal pressure could not be accomplished.

5.4. *Data and Results*

5.4.1. Cylinder Tests

15cm diameter, 30cm in length cylinders were cast in purpose made plastic containers. At the specified times, the concrete was removed from the cylinder by drilling a hole on the bottom and injecting compressed air. After demolding the concrete cylinders compression and slump tests were conducted.

Mix #1 includes: • MaxTen High Performance synthetic macro fibers (MT225300) • 3/4 inch coarse aggregate • Calcium • (Water reducer, fine aggregate, water, other additives TBD)	

Initial morning tests:

Cylinder #1 Cure time: 1h 15m • Cylinder broke internally at the 10'' mark while demolding. • Appears quite wet still however surface has hardened and a cold weld would occur if additional concrete was poured on top. • Compressive strength >2psi (held weight of ~56 pounds)	
Cylinder #2 Cure time: 1h 35m • Cylinder broke internally at the 11'' mark while demolding. • Compressive strength >8psi (held weight of ~226 pounds)	
Cylinder #3 Cure time: 2h 30m • Cylinder came out smoothly from the cylindrical mold. • Compressive strength >11.5psi (held weight of ~330 pounds) but less than 35spi (did not register over 1000 pounds on cylinder compression rig)	
Cylinder #4 Cure time: 3h 15m • Cylinder came out smoothly from the cylindrical mold. • Compressive strength ~35psi (cylinder compression testing rig loaded to 1000 pounds)	
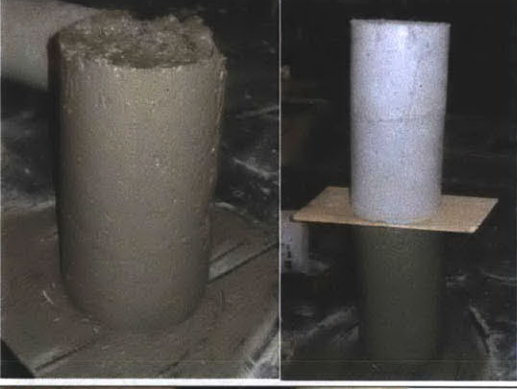
Additional tests were conducted in the afternoon.

Cylinder #5 Cure time: 30m • Still wet. 0 strength.	
Cylinder #6 Cure time: 45m • Some shear strength has developed. • Cylinder held at top, off the ground, in hands. Bottom separated after 20 seconds, breaking bellow hands. Bottom piece of concrete weighed about 20lbs.	
Cylinder #7 Cure time: 1h 20m • More shear strength has developed. • Cylinder held at top, off the ground, in hands. Bottom separated after 20 seconds, breaking bellow hands. Bottom piece of concrete weighed about 28lbs. • It is clear that the samples withstand very small tensile forces before failure.	

Mix #2 includes:
- MaxTen High Performance synthetic macro fibers (MT225300)
- Calcium
- (Water reducer, fine aggregate, water, other additives TBD)

The coarse aggregate was removed to improve flow characteristics. It was observed that, without aggregate, the cure time increases substantially.

Cylinder #1 Cure time: 0h 40m • Completely liquid. Still flows. Will not form cold welds. 0 strength.	
Cylinder #2 Cure time: 1h 30m • Completely liquid. Still flows. Will not form cold welds. 0 strength.	

Three cylinders using mix #2 were broken after curing for 12hours. Compressive strengths were: 78000lbs, 80000lbs, 76000lbs. respectively (~2750 psi)

5.4.2.   Elephant Trunk Flow Test

Mix #1 was dumped from the suspended bucket into the sub-hopper where it funnelled down to a 4inches port. From the 4inches port, it flowed into the 4inches lay-flat hose and on towards the 3inches barbed fitting in the nozzle assembly.

Test #1

The bucket and sub-hopper were too low to the ground and the lay-flat tubing had many kinks in it as it lay on the ground. As concrete flowed into the tubing, it was held up at the kinks with water and smaller particles flowing ahead and the ¾ aggregate jamming together. Once the jam was formed, it moved down the tube as it was un-kinked. As soon as it hit the barbed fitting, it stopped, jamming immediately. It was clear, as soon as the first jam formed, that it would not pass through the fittings.

Test #2

The elephant trunk and nozzle assembly were cleaned out and another attempt was made. This time, the hose was held vertically, entire off the ground; extending straight down from the sub-hopper. When concrete was delivered, it flowed through the nozzle assembly initially but

66

only very slowly. Much slower than it would have come if it weren't catching or beginning to jam. Soon after, it jammed entirely and another slug of ¾ jammed aggregate had formed. The hose was shaken and hit at the jam and water was sprayed up at the jam from below. It remained. The nozzle assembly had to be removed from the lay-flat tubing to be cleaned. However, since the concrete had now sat in the sub-hopper for a minute or two without flowing, another jam of ¾ aggregate formed within the 4inches funnel of the sub-hopper. A metal rod was used to free up the jam from above; a time consuming and cumbersome process.

5.5. Conclusion

The 3inches fittings used in the nozzle assembly were much too small. The 90 degree bend was also very abrupt, again impeding the flow of concrete. It is important that the piping, fittings and the transitions between be as smooth as possible to prevent jamming triggering sites. The concrete must also be kept flowing or the aggregate will settle in any bottlenecks and form jams.

The current thought towards correction is to use:
- At least 4inches fittings for all connections
- Fittings with smoother transitions, e.g. larger radius 90 degree bend or 135 degree
- A mix with smaller aggregate (3/8)
- (Potentially) A mix designed to flow better, trading off cure time.
- (Potentially) A mix with less fibre, trading off strength.

Chp 6. Global ORES Deployment

Site evaluation will play a key role on ORES deployment scenarios, like they do for any other energy harvesting or energy storage system, and should be handled with great care in environment, social and government (ESG) perspectives. Among these three fields ORES will be subject to the similar environmental and governmental but better social reactions. Government regulations, short and long term environmental and social effects should be studied profoundly for ORES deployment however they are beyond the scope of this paper and should be evaluated particularly for each deployment region/scenario since parameters can vary greatly according to states, countries and time being. This paper will mainly evaluate the sites in terms of geography, geology, bottom topography and wind resources and proximity to demand centers.

When searching for appropriate global deployment sites the parameters that play key role are:
1. Depths (200-750m)
2. proximity to population centers (distance from shore 125NM)
3. high wind speeds and wind potential (>7m/s)
4. nearby logistics capabilities (railroads, ports, channels etc.)
5. existing or possible grid connections
6. bottom topography

In order to find the potential deployment sites these criteria were evaluated in merit of order to determine the most economically and technically feasible sites. We started searching for regions where depths are favorable (200-750m) and relatively close to shore (<125NM). Google Earth was used to locate available depths. National reports or data from meteorology agencies of countries were used to preliminary analyze wind potential and wind speeds.

Each region is evaluated individually to give more accurate results. In order to implement this approach global sites are classified as:
1. North America
2. Europe and Mediterranean
3. Asia

During our site evaluation $0.5km^2$/wind turbine projected area, $5MW/km^2$ for offshore wind and 40% capacity factor is assumed [43]. Under the light of these parameters possible global deployment sites according to regions are studied in following section and possible corresponding potential will be stated.

6.1. North America

Our initial research started with North America; Gulf of Maine, Gulf of Mexico, San Diego, Los Angeles, San Francisco, and Hawaii. According to a National Renewable Energy

68

Laboratory report offshore wind potential of US in 90 hub height and bathymetric depths are shown in Figure 42 and Figure 43 respectively [43].
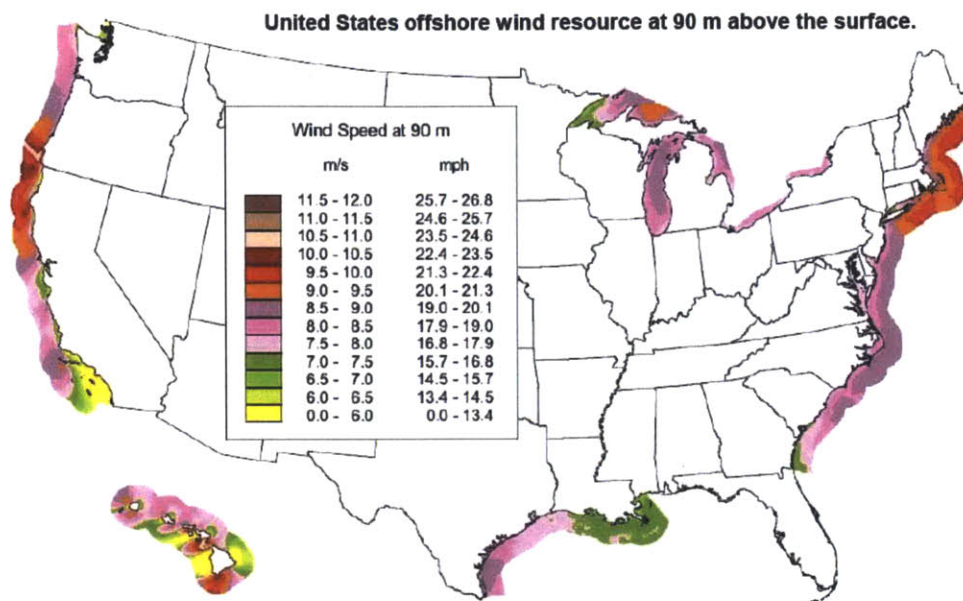
Figure 42 Offshore wind potential of US at 90m height (source: [43])
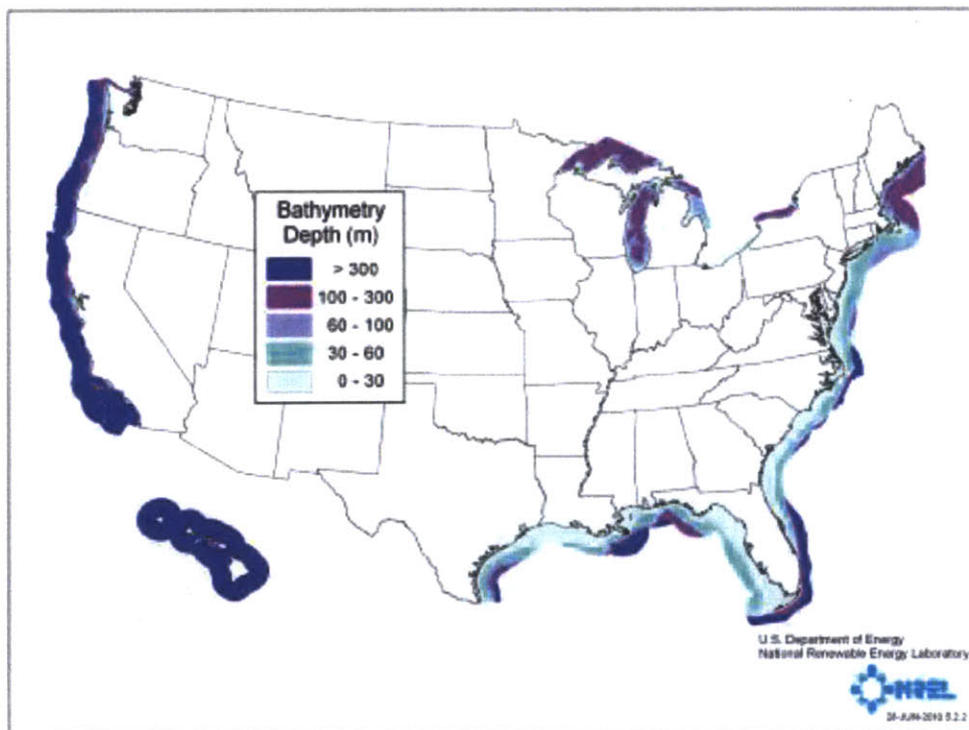
Figure 43 US coast bathymetric chart (source: [43])

Figure 43 shows that among these potential deployment sites in US, Gulf of Maine and Los Angeles offers better wind profile. However 300-700m depths are 200NM away from the shore in Gulf of Maine. Conversely greater depths are closer to shore on the west coast but wind resources are lower except San Francisco 200-750m depths are within 2-10NM range in the west coast.

Figure 44 Gulf of Maine ORES deployment site. Total surface are available for ORES deployment is 2,230km²

Figure 45 New York and New Jersey ORES deployment site. Total surface area in 200-750m depths range is 1,000km²

Figure 46 ORES on south east US, Florida, South Carolina. Total surface area is 41,160km²
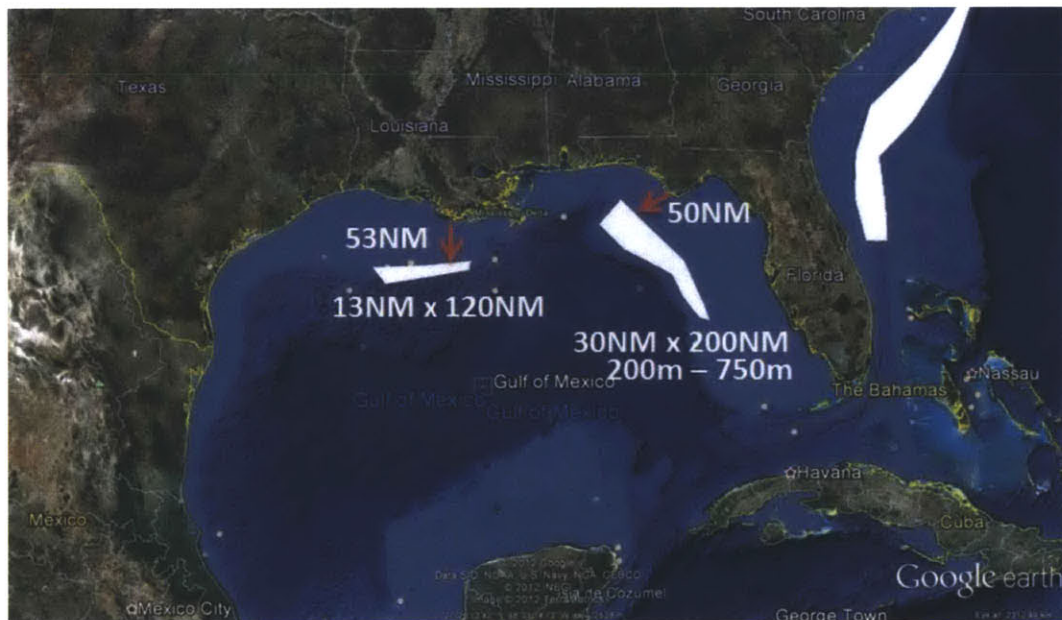
Figure 47 Regions available for possible ORES deployment in Gulf of Mexico have a total of 25,929km² surface area, and 50NM away from shore
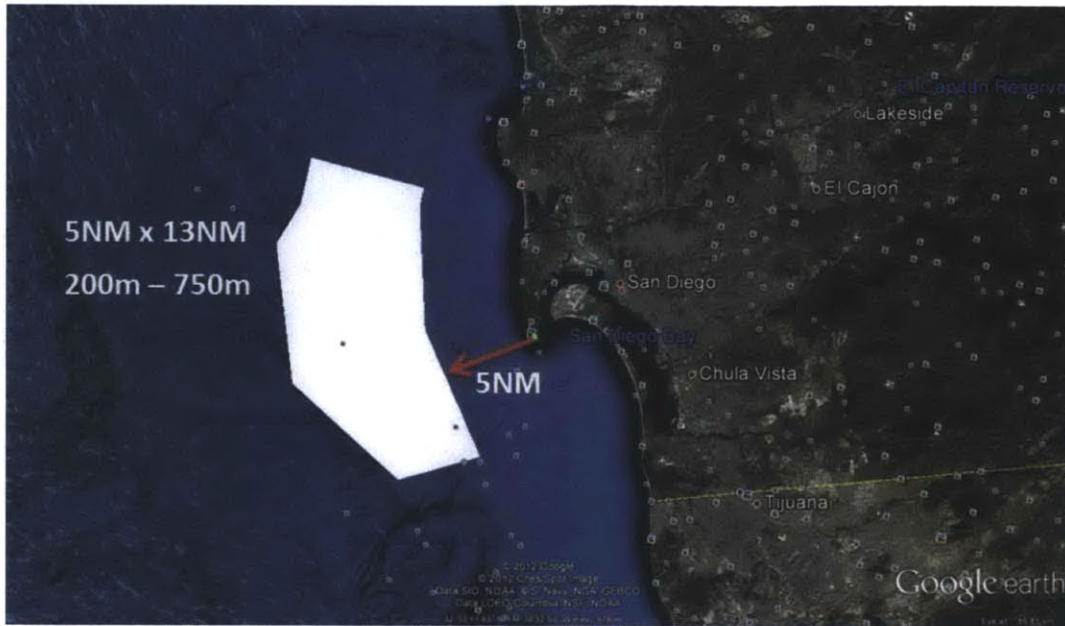
Figure 48 San Diego ORES deployment site has a total of 223km² surface area with depths ranging 200-750m and is 5NM away from shore

Figure 49 Los Angeles possible deployment sites have 2263km² 2NM away and 257 km² 15NM away from shore
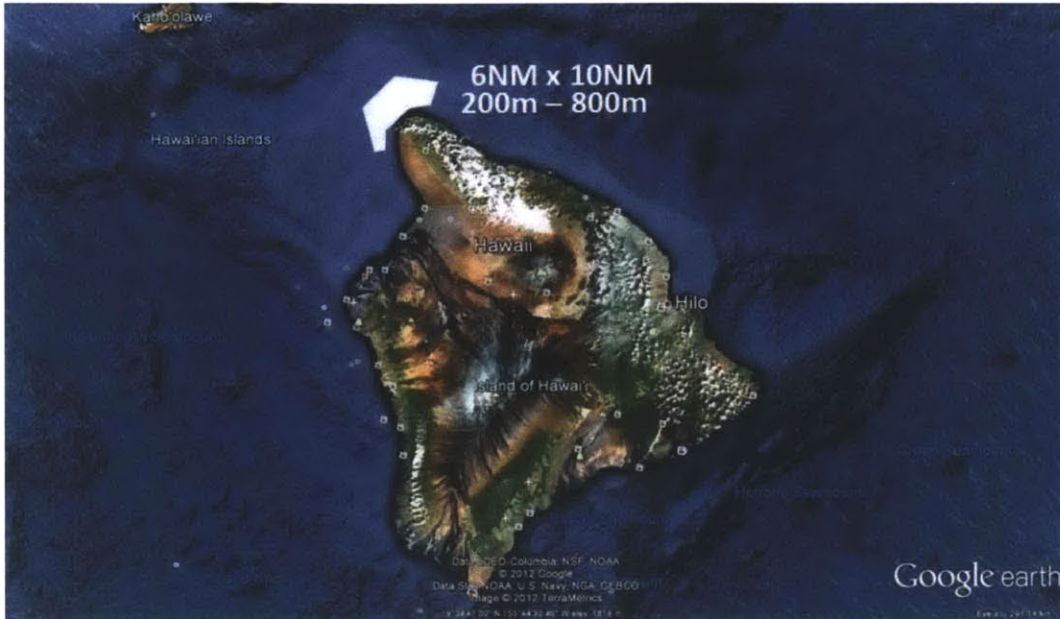
Figure 50 Possible Hawaii deployment site is 2NM away from shore and has a 206km^2 surface area

6.2. Europe, Mediterranean and Aegean Sea

High oil prices, lack of fossil fuel resources, instability on the upstream of the NG and binding goals of Kyoto Protocol (accepted by EU in 2005) pushed EU countries to implement measures to maintain or decrease their Greenhouse Gas (GHG) emissions. Most of EU countries, led by Denmark, Germany, Spain and UK, started to increase their renewable energy portfolio in order to grant their energy security while satisfying growing energy demand. Solar PV and wind account for 96% of renewable energy installations in 2011. 9,196 MW of name plate capacity wind power was installed in 2011 which adds up to 94 GW of total capacity [44]. 6 out of 10 most aggressive global wind investments are accomplished by EU countries. Top 10 worldwide wind investments are shown in Table 9.

Table 9 Top ten wind installations around the world

Countries	Installed Capacity (MW)	Capacity Increase Percentage in 2010 (%)	Capacity Increase (MW) in 2010
China	42,287	21.8	16,510
USA	40,180	20.7	5,201
Germany	27,214	14	1,493
Spain	20,676	10.6	1,516
India	13,065	6.7	2,139
Italy	5,797	3	948
France	5,660	2.9	1,086
England	5,204	2.7	962
Canada	4,009	2.2	690
Denmark	3,752	2.2	327
Leading 10	**167,844**	**86.3**	**33,471**
Rest of the World	**26,546**	**13.7**	**3994**
World Total	**194,390**	**100**	**37,466**

The share of Europe in worldwide offshore wind installations is even higher. Table 10 shows that 8 out of 10 largest offshore capacity is installed by EU countries.

Table 10 Global offshore wind installations

Country	2008 Installed Off Shore Capacity (MW)
U.K.	1041
Denmark	664
Netherlands	247
Sweden	163
China	102
Germany	72
Finland	30
Belgium	30
Ireland	25
Others	7

Existing wind power installations utilize monopole wind turbine technology thus farther distances with higher wind potential have not been utilized yet. As more research is conducted on FWTs new opportunities will arise and we believe there will be a major boost in the wind

installations. Figure 51, showing onshore and offshore wind installations in Europe, supports our prediction.

There is an increase in offshore installations since 2000. The spike in 2002 and 2003 is due to thigh installations accomplished by Denmark. After witnessing Denmark's success more countries started to make investment since 2007. Same will also be applied to FWTs. Denmark, Japan and UK are among the countries which are currently working on FWTs that can be deployed at 50-100m depths. Wind industry for the developed grids is waiting for the real world applications for further large scale investment.

OFFSHORE'S SHARE OF ANNUAL EU WIND POWER MARKET (MW)   FIGURE 3.4
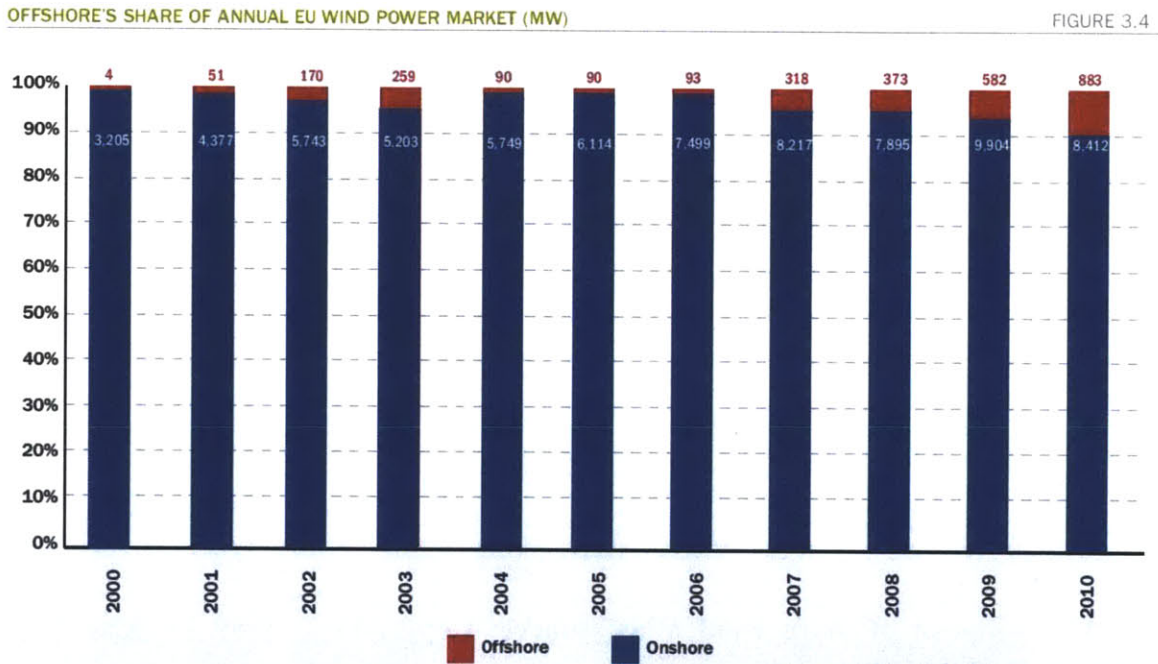
Figure 51 Onshore and offshore wind installations in Europe (source:[44])

European offshore wind atlas is shown in Figure 52. The atlas was created by Riso National Laboratory, Denmark with Wind Atlas Analysis and Application Program (WAsP). WAsP is a climate prediction program which was developed by DTU Wind Energy [45].

Wind resources over open sea (more than 10 km offshore) for five standard heights										
	10 m		25 m		50 m		100 m		200 m	
	ms^{-1}	Wm^{-2}	ms^{-1}	Wm^{-2}	ms^{-1}	Wm^{-2}	ms^{-1}	Wm^{-2}	ms^{-1}	Wm^{-2}
	> 8.0	> 600	> 8.5	> 700	> 9.0	> 800	> 10.0	> 1100	> 11.0	> 1500
	7.0-8.0	350-600	7.5-8.5	450-700	8.0-9.0	600-800	8.5-10.0	650-1100	9.5-11.0	900-1500
	6.0-7.0	250-300	6.5-7.5	300-450	7.0-8.0	400-600	7.5- 8.5	450- 650	8.0- 9.5	600- 900
	4.5-6.0	100-250	5.0-6.5	150-300	5.5-7.0	200-400	6.0- 7.5	250- 450	6.5- 8.0	300- 600
	< 4.5	< 100	< 5.0	< 150	< 5.5	< 200	< 6.0	< 250	< 6.5	< 300

Figure 52 European offshore wind atlas (source: Copyright © 1989 by Risø National Laboratory, Roskilde, Denmark)

Preliminary analysis on continent Europe and Mediterranean shows that northwestern part of Europe, Bay of Biscay, north Mediterranean and east Aegean Sea have higher wind potentials. However despite having the highest wind potential North Sea, the region between the west UK and east of Norway, is shallow for deployment, having depths ranging from 10-110m. West of UK, southern France, and western Turkey have great wind potential with favorable depths and shorter distances to the shore.

Figure 53 Western Europe has two possible deployment sites a total of 3086km^2 and 20 to 100NM away from shore
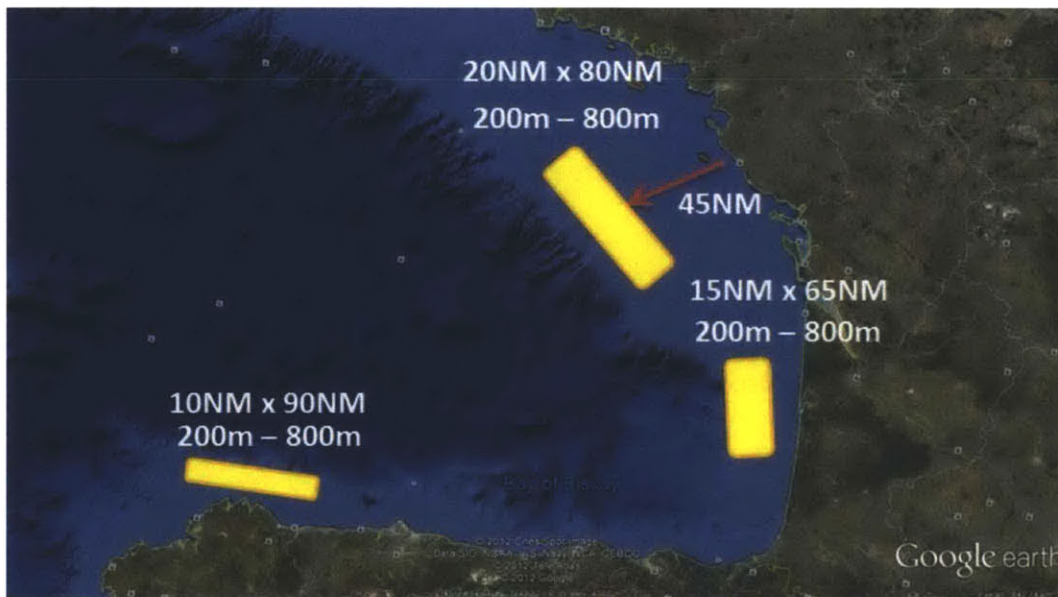
Figure 54 Bay of Biscay deployment site

Northern sea has gained considerable attention recently due to the long lasting success of offshore installations by Denmark. Furthermore North Sea Offshore Grid is being built by European Union to encourage more offshore wind installations. However because of the shallow depths it is not available for ORES deployment. Western Europe and northern Bay of Biscay have great potential for FWT installations. Wind speeds at 90m hub height in these regions are expected to be more than 8m/s with a 650-1000W/m^2 wind potential. The primary advantage of

these two regions is the proximity to big demand centers which aim to increase their renewable energy portfolio while necessitating a higher quality grid.
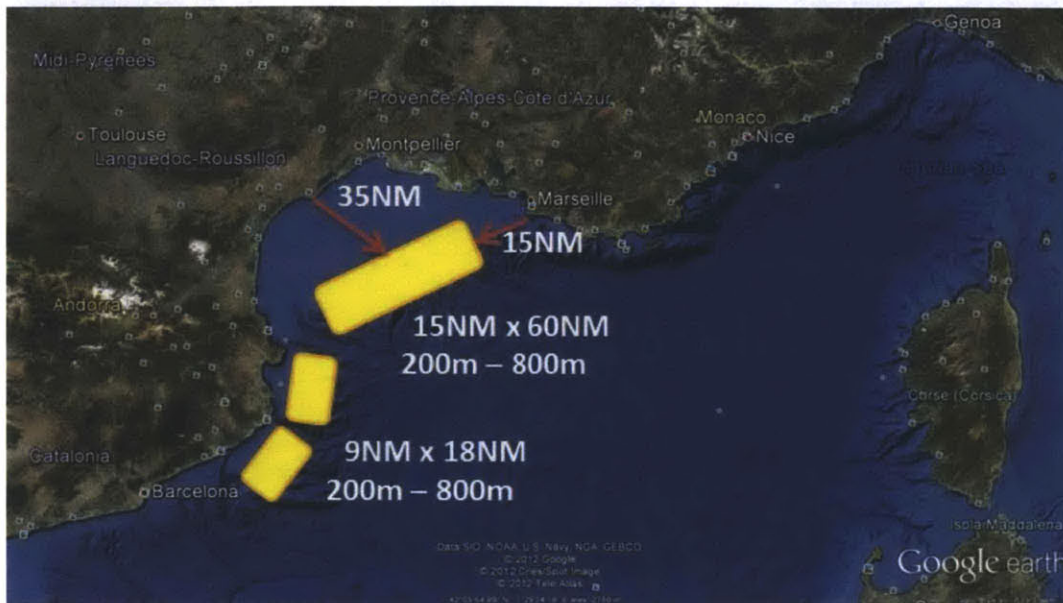
Figure 55 North Mediterranean deployment opportunities

Both France and Spain installed more than 2,500MW nameplate capacity wind in 2010 most of which was on-land installations. Projected regions in Figure 55 are close to demand centers however they are also touristic regions. In order to avoid a strong opposition from local and global communities a solution can be creating a storage farm directly attached to the grid to improve grid quality.

Figure 52and Figure 56 show that eastern Aegean Sea has also high wind speeds and wind potential. Turkish wind atlas was created by Turkish State Meteorological Service by using the same software which was used to create European Wind Atlas, WAsP.
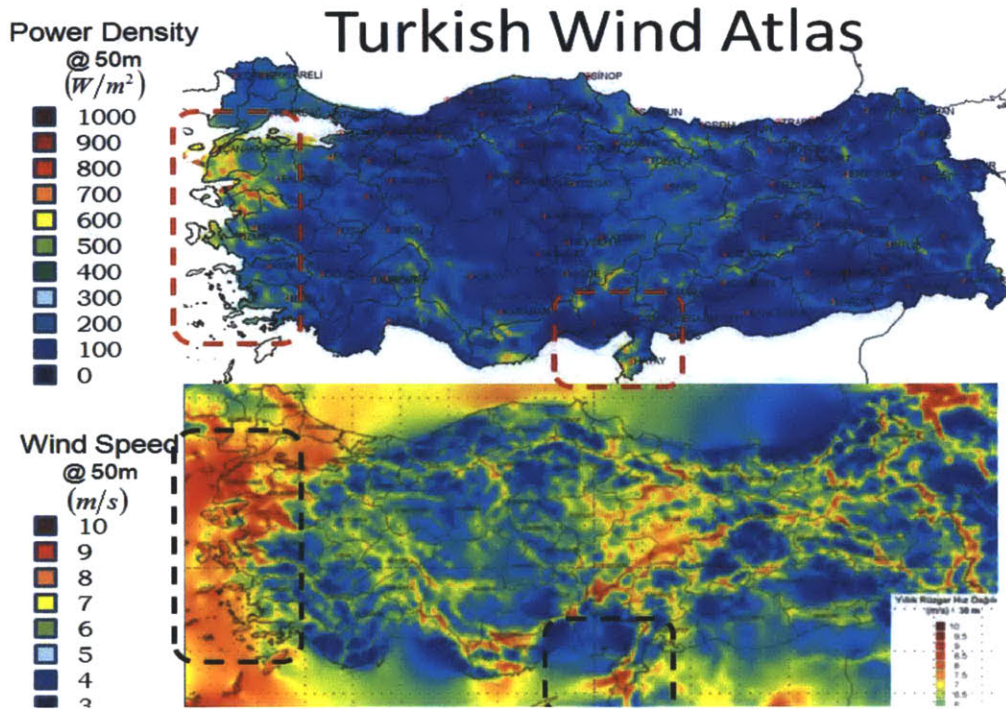
Figure 56 Turkish Wind atlas (power density at the top and wind speed at the bottom) (source: www.dmi.gov.tr)

In addition to Aegean Sea a deployment in the south east coast of Turkey, Hatay region is economically feasible. Depths range from 200-1000m 45NM away from shore. Istanbul has also great potential for deployment in Black Sea coast but due to its strategic importance such deployment seems not likely to happen in the near future.
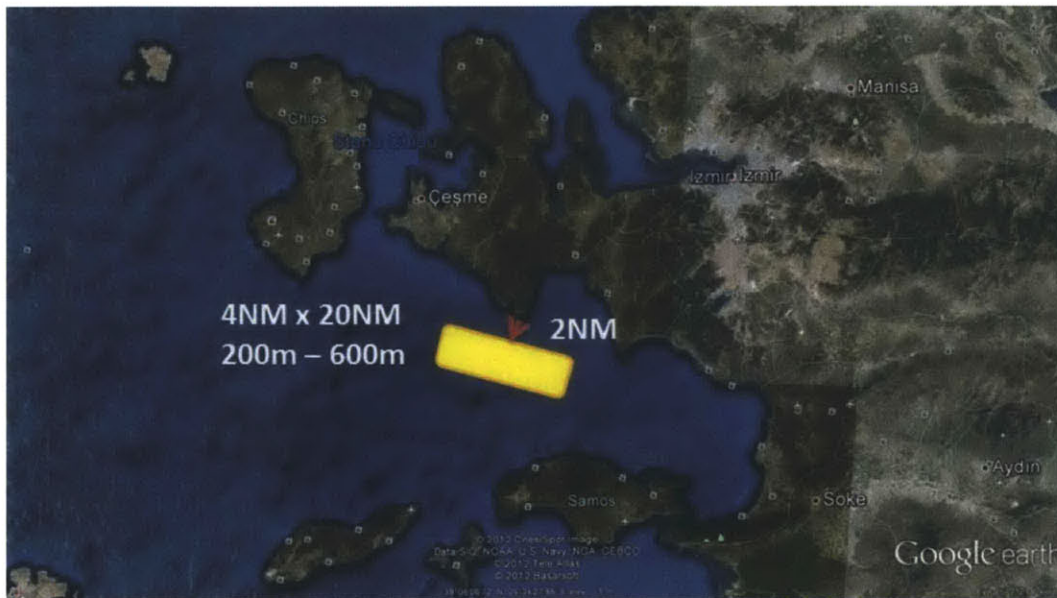
Figure 57 Western Aegean Sea, Kusadasi Bay, Izmir deployment site (Turkey)
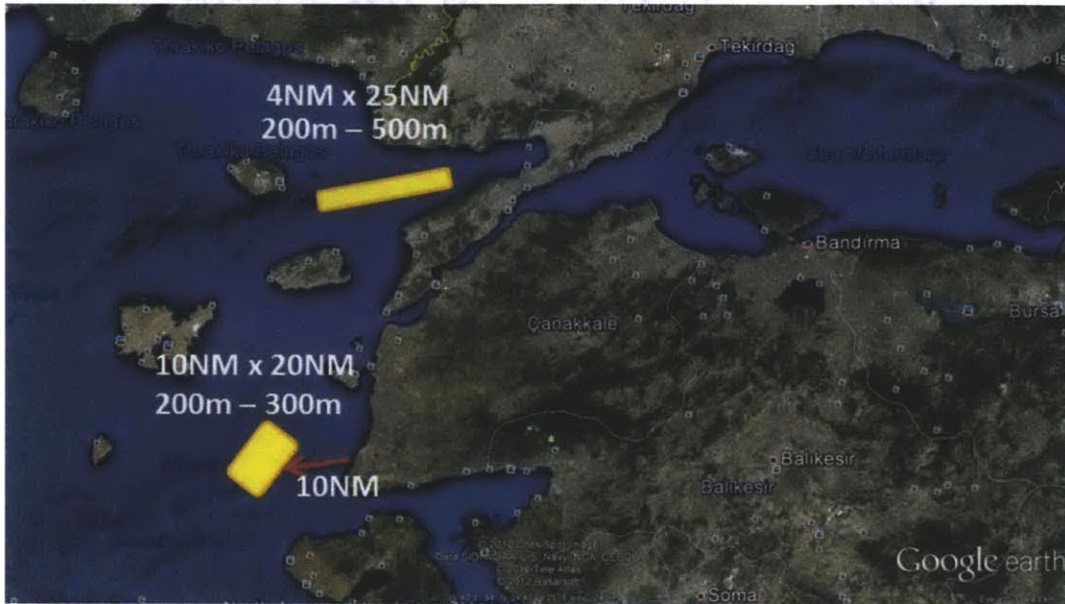
Figure 58 Saros Bay and Balikesir deployment site (Turkey)

Figure 59 Eastern Mediterranean, Iskenderun Bay deployment site (Turkey)

6.3. Asia

After the Tohoku earthquake on 11 March 2011, followed by tsunami and Fukushima disaster the public opinion about the use of nuclear has changed dramatically and shifted to decrease the share of nuclear in Japan's electricity supply. Japan hit by the great earthquake and lost most of its power after the event still needs to provide energy to sustain its industry.

However with the increasing domestic and global public opposition against nuclear power, Japan officials announced their plans of investing in wind power by building the world's first floating wind farm [46]. Our previous studies focused on Tokyo and Hokkaido however after the earthquake we expanded our focus to evaluate the regions near existing nuclear plants. By this way existing grid connections can be utilized and new investment in infrastructure can be avoided. Existing nuclear plants in Japan are shown in Figure 60 and listed in Table 11.
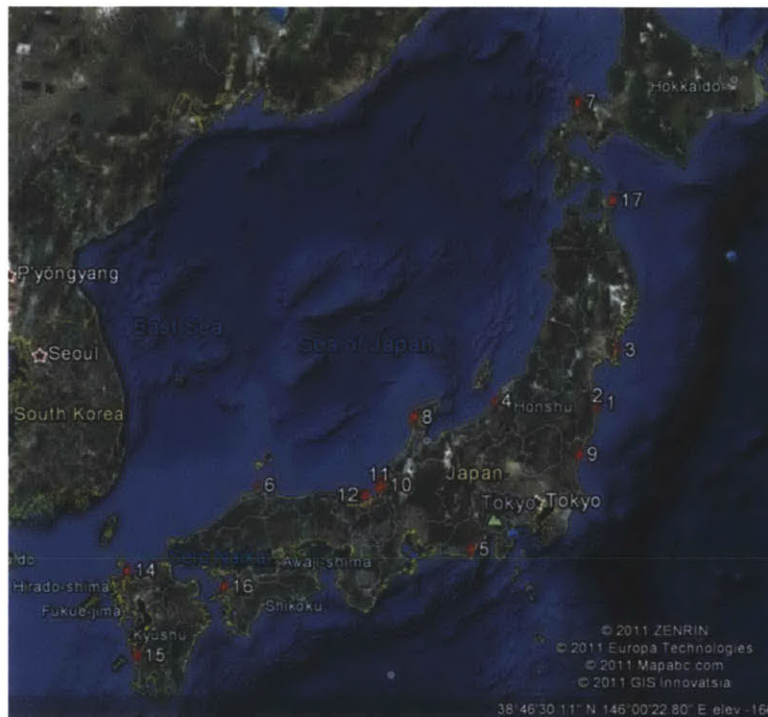
Figure 60 Nuclear plants in Japan

Table 11 Nuclear plants in Japan (credit: Brian Hodder)

Map ID#	Installation Name	Net Capacity (MW)	Latitude	Longitude
1	Tokyo Electric-Fukushima-Daiichi	4,696	37°25'22.7"N	141°01'58.5"E
2	Tokyo Electric-Fukushima-Daini	4,400	37°18'59"N	141°1'32"E
3	Tohoku Electric-Onagawa	8,212	38°24'04"N	141°29'59"E
4	Tokyo Electric-Kashiwazaki-Kariwa	2,174	37°25.7'N	138°36.1'
5	Chubu Electric-Hamaoka	3,617	34°37'25"N	138°08'33"E
6	Chugoku Electric-Shimane	1,280	35°32'18"N	132°59'57"E
7	Hokkaido Electric-Tomari	2,070	43°2'10"N	140°30'45"E
8	Hokuriku Electric-Shika	1,746	37°03'40"N	136°43'35"E
9	Japan Atomic Power-Tokai Daini	1,100	36°27'59"N	140°36'24"E
10	Japan Atomic Power-Tsuruga	1,517	35°45'7"N	136°1'8"
11	Kansai Electric-Mihama	1,666	35°42'12.51"N	135°57'48.88"E
12	Kansai Electric-Ohi	4,710	35°32'28.35"N	135°39'14.74"E
13	Kansai Electric-Takahama	3,392	35°31'19.17"N	135°30'14.24"E
14	Kyushu Electric-Genkai	3,478	33°30'56"N	129°50'14"E
15	Kyushu Electric-Sendai	1,780	31°50'01"N	130°11'23"E
16	Shikoku Electric-Ikata	2,022	33°29'27"N	132°18'41"E
17	Tohoku Electric-Higashidori	1,100	41°11'17"N	141°23'25"E

Japan's population is 128 million and has a land area of 377,915 km². It has the third largest economy in the world [47]. Since most of the land is used for urbanization (87%) and agriculture (11.6%) there is not enough land for building power plants with less power density such as PV or solar thermal. As a result of this constraint offshore wind provides promising future for replacing the nuclear plant while not using land area. Promising regions with favorable depths around Fukushima are shown in Figure 61. The area enclosed in green line is 5,140 km² and 50km away from the coast.

1 Tokyo Electric - Fukushima Daichi
2 Tokyo Electric - Fukushima Daini
3 Tohoku Electric - Onagawa
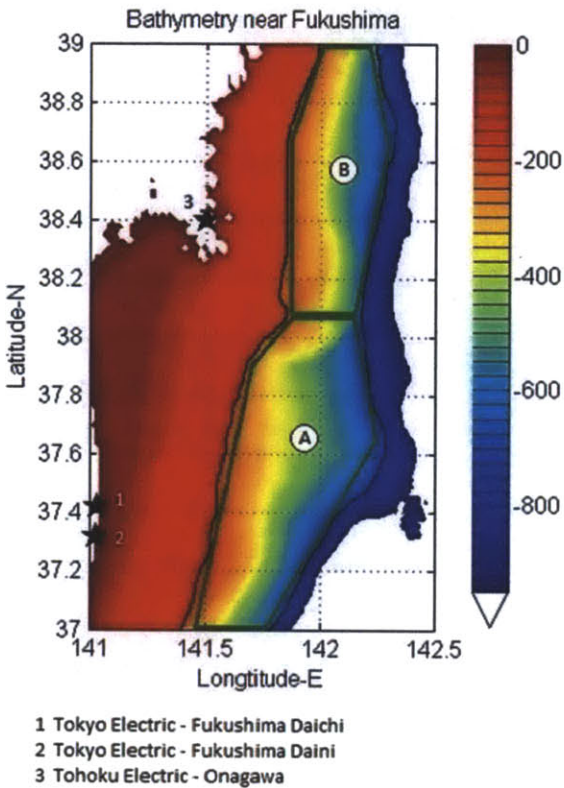
Figure 61 Bathymetry near Fukushima

Chubu nuclear plant is located on the south east of Japan. Bottom topography around the plant and Hamaoka is uneven and broken with underwater cliffs. East of the nuclear plant lies Suruga Canyon and this makes a possible deployment technically challenging. Figure 62 shows the bathymetry near Chubu nuclear plant near Hamaoka. Distances of possible deployment site is relatively closer to the shore and studied area represents for 34 km².
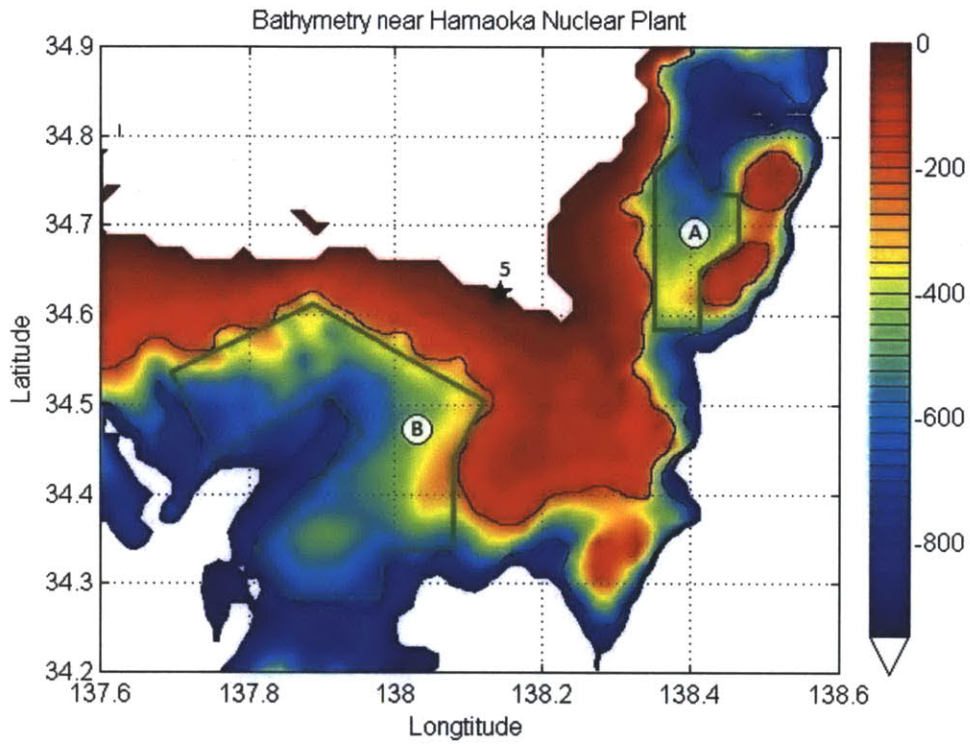
Figure 62 Bathymetry near Chubu Electric - Hamaoka
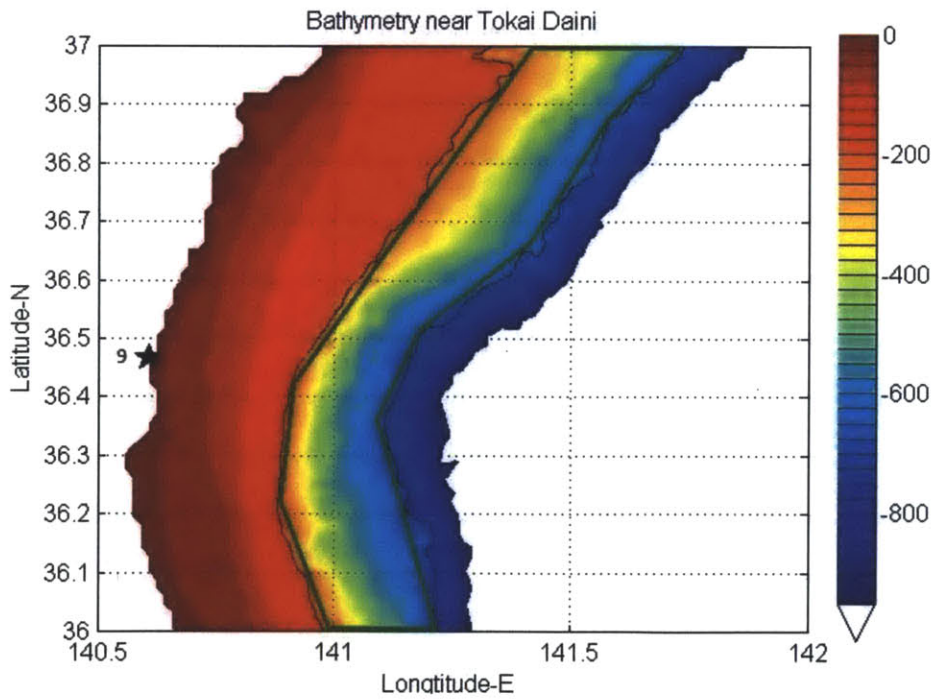
Figure 63 Bathymetry near Tokai Daini plant

Figure 63 shows that there is a relatively smoother terrain on the east coast of Japan near Tokai Daini power plant operated by Japan Atomic Power. The available region east of the plant has 2,500 km^2 of surface area hence is encouraging for ORES deployment.

The last region studied in Japan is the west of Sendai plant near Kyushu. A total of 12,300 km^2 is available for ORES deployment but further research should be conducted to better understand use conflict with fisheries. Figure 64 shows the region evaluated for deployment near Kyushu.
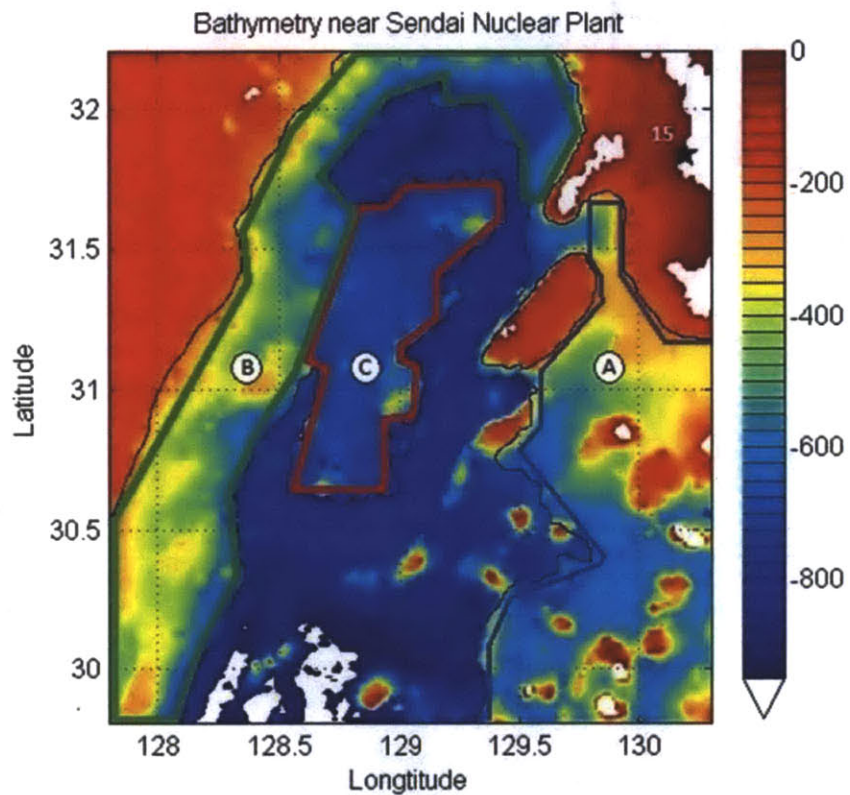
Figure 64 Bathymetry near Sendai Nuclear plant, Kyushu

Chp 7. Concluding Remarks

7.1. Design Assessment

Design and manufacturing methods of ORES has been extensively studied and represented in this thesis. Because of the simplicity of the concept the real life application of underwater energy storage is only a matter of engineering. Oil and gas industry has been successfully dealing with underwater platforms and harsh marine environment for decades. Because of the high safety standards and complexity of the industry a wide range of equipment which can ease ORES deployment has been developed. Leveraging already existing technology, early stage deployment can start with easy-to-manufacture geometry without additional features.

According to our calculations and simulations sphere has energy density, capacity and material advantages compared to tubes. Using the same amount of cement, fly ash and steel, spheres have a higher energy capacity. However manufacturing and transporting full-scale 27m ID sphere remains technically challenging and not possible in most of the deployment sites with the current port capabilities.

On the other hand tubes are easy to manufacture and transport. They can be cast in segments and are scalable to have higher capacities simply by adding multiple pieces together or stacking them up. In this scenario having a long tube network under the ocean is highly dependent on the bottom topography while stacking the tubes up is challenging due to the underwater currents. Because of the wide surface area of the tubes even a small current can act great forces which can misalign the connections leading to a total system failure. Sealing the connection between the tubes is also a challenge. In spherical approach each piece is enough to provide more than 10MWh energy storage (depending on the depth and the diameter) and there are less mating surfaces. However to reach the same amount of storage capacity more than 1 pipe is required thus there are more critical points in the overall system. In addition energy density with respect to the used material is lower compared to the spheres as well.

The main advantage of the ORES concept is regardless of the shape or geometry of the structure, energy can be stored under the water without having complex features. The capacity is scalable and can be increased by simply deploying more units. Furthermore each unit is also capable of working independently providing initiative for the system operators to dispatch according to changing demand on the grid. A reversible turbine (which can act both as a turbine and a pump, i.e. Francis turbine) will be installed on the system which has a very short ramp-up time and can start generating electricity in minutes. The ability of fast response rate and short startup time increases the value of storage and enables renewables, especially wind, to meet peak demand.

7.2. Zorb Ball and Concrete Test Results

In our experiments due to the superior material properties TPU was selected to be used in Zorb ball. We witnessed that ball can carry its own weight and maintains its spherical form almost perfectly if properly pressurized. However, when a person gets in the ball it starts deforming its shape elastically, and forms a flat surface at the bottom where the ball contacts the ground. Based on this observation additional measured should be taken to maintain the spherical form during the continuous pouring. Straps tightly tied in a spherical pattern surrounding the ball or plates should be used to help support the weight of the concrete to keep the sphere shape unless concrete is poured very slowly which forms cold joints resulting in strength loss.

We learned greatly during our field trips and experiments at American Concrete, MN. Our tests with concrete and equipment we used show that 3/4 inch aggregate size is big for 4inch pipes, sub-hopper and elephant trunk resulting in clogging. In addition to the aggregate size glass fiber in the cement mix also increases the likelihood of clogging. However when either glass fiber or big size aggregate is removed from the mix this results in strength loss or increased curing time. It is concluded from the experiments and field observations that larger size pipes and connections should be used in order not to compromise the structural strength.

Field trip to American Concrete, MN, and quote from the Project Manager (PM) revealed the fact that costs of manufacturing spike without a dedicated plant; mainly because the custom manufacturing process interrupts the ongoing business of the company. Even though initial project expenses were calculated in detail in accordance with the PM, contingencies affected the decisions of the company resulting in four times more costs putting ORES project out of budget[2].

7.3. Further Study and Next Steps

ORES team has been studying the design, manufacturing methods, worldwide deployment opportunities extensively for more than 4 years. We made our calculations, produced lab-size prototypes, manufactured first scaled 90cm prototype and tested it on land. We made preliminary analysis of almost every coast of the countries which has potential for a possible ORES deployment. However there is still a lot to be accomplished before a full-scale ORES unit goes operational.

A 3m ID sphere or an equivalent concrete structure should be cast and deployed at sea to prove the engineering skills are capable of working the ORES concept. During the next prototype rotating equipment on the shelf can be used since it is not going to be a mass production. This step will be crucial and exciting as it is going to be the first offshore prototype.

---

[2] Please refer to Appendix for detailed initial budget

There will be a lot to learn in the marine experiments which will enlighten the manufacturing process, full-scale deployment, and even change the direction of the project.

As MIT's motto states, "Mens et Manus", "Mind and Hand" our vision is to create value from this energy storage from which humankind can benefit. In order to achieve this goal collaborations and partnerships which can make this vision to come true should be constituted. Partnership with utility companies should be established to help them improve grid quality, allowing higher rates of renewable energy usage while ensuring energy security.

Chp 8.   References

[1]   Bloomberg New Energy Finance and Frankfurt School UNEP Collaborating Centre for Climate & Sustainable Energy Finance, *GLOBAL TRENDS IN RENEWABLE ENERGY INVESTMENT 2011*. 2011.

[2]   W. Musial and B. Ram, "Large-Scale Offshore Wind Power in the United States," 2010.

[3]   K. Michael, "Utilities See Another Peak Power Hour Evolve - and Technology Responds," *Seeking Alpha*, pp. 17-18, 12-Oct-2008.

[4]   P. Denholm, M. Milligan, E. Ela, and B. Kirby, "The Role of Energy Storage with Renewable Electricity Generation," 2010.

[5]   CAISO, "California ISO Open Access Same-time Information System." [Online]. Available: http://oasis.caiso.com. [Accessed: 04-Apr-2012].

[6]   A. Mills, R. Wiser, and K. Porter, "The Cost of Transmission for Wind Energy : A Review of Transmission Planning Studies," 2009.

[7]   J. Eyer and G. Corey, "Energy Storage for the Electricity Grid : Benefits and Market Potential Assessment Guide," 2010.

[8]   "Electricity Storage Association," 2008. [Online]. Available: http://www.electricitystorage.org/technology/storage_technologies/technology_compariso n. [Accessed: 20-Apr-2011].

[9]   Energy Information Administration, "International Energy Statistics," 2012. [Online]. Available: http://www.eia.gov/cfapps/ipdbproject/iedindex3.cfm?tid=2&pid=82&aid=7&cid=regions &syid=2008&eyid=2010&unit=MK. [Accessed: 11-Apr-2012].

[10]   European Comission, "European Energy pocket book," 2010. [Online]. Available: http://ec.europa.eu/energy/publications/doc/statistics/part_2_energy_pocket_book_2010.p df. [Accessed: 11-Apr-2012].

[11]   Energy Information Administration, "An Updated Annual Energy Outlook 2009 Reference Case Reflecting Provisions of the American Recovery and Reinvestment Act and Recent Changes in the Economic Outlook," 2009.

[12]   W. Peng and D. Chen, "Some considerations on the development of Pumped Hydroelectric Storage power station in China," People's Republic of China, 2010.

[13] The Federation of Electric Power Companies of Japan, "ELECTRICITY REVIEW JAPAN," 2012.

[14] V. Marano, G. Rizzo, and F. A. Tiano, "Application of dynamic programming to the optimal management of a hybrid power plant with wind turbines, photovoltaic panels and compressed air energy storage," *Applied Energy*, Feb. 2012.

[15] "E.ON-Kraftwerk Wilhelmshaven - Portrait." [Online]. Available: http://www.kraftwerk-wilhelmshaven.com/pages/ekw_en/Huntorf_Power_Plant/Portrait/index.htm. [Accessed: 17-Apr-2011].

[16] F. Crotogino, K. B. B. Gmbh, K.-uwe Mohmeyer, R. Scharf, and E. O. N. K. Bremen, "Huntorf CAES : More than 20 Years of Successful Operation by," *Spring 2001 Meeting*, no. April, 2001.

[17] "CAES < McIntosh Power Plant < Generation < Energy Resources < PowerSouth Energy Cooperative." [Online]. Available: http://www.powersouth.com/mcintosh_power_plant/compressed_air_energy. [Accessed: 17-Apr-2011].

[18] "How much electricity does an American home use? - FAQ - U.S. Energy Information Administration (EIA)." [Online]. Available: http://www.eia.gov/tools/faqs/faq.cfm?id=97&t=3. [Accessed: 21-Mar-2012].

[19] "ESPC Adiabatic CAES Process," 2011. [Online]. Available: http://www.espcinc.com/mobile/index.php?option=com_k2&view=item&id=10:caes-adiabatic&Itemid=3. [Accessed: 17-Apr-2011].

[20] "RWE AG - ADELE – Adiabatic compressed-air energy storage (CAES) for electricity supply," 2011. [Online]. Available: http://www.rwe.com/web/cms/en/365478/rwe/innovations/power-generation/energy-storage/compressed-air-energy-storage/project-adele/. [Accessed: 17-Apr-2011].

[21] By Liz Enbysk and SGN Managing Editor, "Toronto startup goes underwater with compressed air energy storage." [Online]. Available: http://www.smartgridnews.com/artman/publish/Technologies_Storage/Toronto-startup-goes-underwater-with-compressed-air-energy-storage-4583.html. [Accessed: 20-Mar-2012].

[22] "Underwater Compressed Air Electrical Storage." [Online]. Available: http://hydrostor.ca/home/. [Accessed: 21-Apr-2012].

[23] "In der Tiefe der Meere: Hohlkugeln speichern überschüssigen Windstrom - Umwelt & Technik - FAZ." [Online]. Available: http://www.faz.net/aktuell/technik-motor/umwelt-technik/in-der-tiefe-der-meere-hohlkugeln-speichern-ueberschuessigen-windstrom-1608012.html. [Accessed: 17-Apr-2011].

[24] "where to store wind-powered energy? under water! - cnn.com." [Online]. Available: http://edition.cnn.com/2008/TECH/science/03/31/windpower/. [Accessed: 24-Apr-2012].

[25] A. S. Greenlee, "Design of Subsea Energy Storage Chamber By Design of Subsea Energy Storage Chamber," Massachusetts Institute of Technology, 2009.

[26] G. E. Fennell, "System Design and Manufacturability of Concrete Spheres for Undersea Pumped Hydro Energy or Hydrocarbon Storage," Massachusetts Institute of Technology, Cambridge, 2011.

[27] A. H. Slocum, G. E. Fennell, and A. S. Greenlee, "Offshore Energy Harvesting, Storage, and Power Generation System," U.S. Patent US 2011/0215650 A12011.

[28] D. Steward, G. Saur, M. Penev, and T. Ramsden, "Lifecycle Cost Analysis of Hydrogen Versus Other Technologies for Electrical Energy Storage," 2009.

[29] W. Musial, S. Butterfield, and A. Boone, "Feasibility of Floating Platform Systems for Wind Turbines Preprint," *Symposium A Quarterly Journal In Modern Foreign Literatures*, no. November 2003, 2004.

[30] A. H. Slocum, G. E. Fennell, G. Dündar, B. G. Hodder, J. D. C. Meredith, and M. Sager, "Ocean Renewable Energy System (ORES) – Analysis of an Undersea Energy Storage," *IEEE Marine Energy and Environment*, no. On press, 2012.

[31] B. Balboni and J. Chiang, *RS Means estimating handbook*, 3rd Editio. Kingston: Wiley, 2010.

[32] H. C. H. Darley and G. R. Gray, *Composition and Properties of Drilling and Completion Fluids*, 5th Editio. Houston, TX: Butterworth-Heinemann, 1988.

[33] J. S. Hanor, "Barite-Celestine Geochemistry and Environments of Formation," *Reviews in Mineralogy and Geochemistry*, vol. 40, no. 1, pp. 193-275, Jan. 2000.

[34] "Global Steel Prices," 2012. [Online]. Available: http://www.worldsteelprices.com/. [Accessed: 16-Mar-2012].

[35] "American Shotcrete Association." [Online]. Available: http://www.shotcrete.org/. [Accessed: 12-Jan-2012].

[36] Skanska, "Skanska - Submerged Tunnel at Bjørvika (center of Oslo)," 2008. [Online]. Available: http://www.skanska.com/en/Projects/Project/?pid=2006&plang=en-us.

[37] "Yantai Raffles' world-record gantry crane should see first lift this year - Offshore." [Online]. Available: http://www.offshore-mag.com/articles/print/volume-68/issue-6/cranes-hoists-and-winches/yantai-rafflesrsquo-world-record-gantry-crane-should-see-first-lift-this-year.html. [Accessed: 12-Feb-2012].

[38]   J. D. C. Meredith, "Design , Construction and Testing of an Ocean Renewable Energy Storage Scaled Prototype," Massachusetts Institute of Technology, 2012.

[39]   "ZORB.com - ZORB Rotorua." [Online]. Available: http://www.zorb.com/zorb/rotorua/. [Accessed: 09-May-2012].

[40]   "Elastollan - The high performance TPU." [Online]. Available: http://www2.basf.us/urethanechemicals/tpu/tpu_properties.htm. [Accessed: 02-Apr-2012].

[41]   A. K. Schindler and B. F. Mccullough, "The Importance of Concrete Temperature Control During Concrete Pavement Construction in Hot Weather Conditions," 2002.

[42]   F. M. White, *Fluid Mechanics*. McGraw Hill, 2003, p. 362.

[43]   M. Schwartz, D. Heimiller, S. Haymes, and W. Musial, "Assessment of Offshore Wind Energy Resources for the United States," 2010.

[44]   European Wind Energy Association, "Wind in power," 2011.

[45]   R. D. N. for B. Energi, "Welcome to WAsP!," Apr. 2012.

[46]   "Updated: Fukushima hopes 'world's first floating offshore wind farm' will spark post-tsunami recovery."[Online]. Available: http://www.businessgreen.com/bg/news/2157517/fukushima-hopes-worlds-floating-offshore-wind-farm-spark-post-tsunami-recovery?goback=%2Egde_2632479_member_99841487. [Accessed: 10-Mar-2012].

[47]   "CIA - The World Factbook, Japan." [Online]. Available: https://www.cia.gov/library/publications/the-world-factbook/geos/ja.html. [Accessed: 28-Apr-2012].

Chp 9. Appendix

9.1. Bill of Materials (BOM)

Table 12 Bill of Materials and cost estimation for 3m ORES prototype

	Properties		Serial no	Qty	Unit price	Total price
Sphere					$	$
Zorb	3m ID, 3.6m OD	Jump Balloons	-	1	2,025.00	2,025.00
Bulkhead fittings	3" Female NPT (both sides)	US Plastic Corp	32228	10	25.35	253.50
Knife Gate Valve	3" M-NPT x F-NPT	McMaster	3999K37	10	54.22	542.20
Concrete Dispenser						
Suspended sub-hopper		Gar-Bro Mfg				
Collar		Gar-Bro Mfg				
Elephant trunk		Gar-Bro Mfg				
Clamp		Gar-Bro Mfg		1	1,485.00	1,485.00
Pipe stub	3" barb to M-NPT	McMaster	5218K42	1	6.04	6.04
Ball Valve	Plastic w/ union. 3" F-NPT	McMaster	4953K717	1	135.06	135.06
Nipple	3" NPT	McMaster	4882K49	1	8.64	8.64
Lifting equipment						

Slings	25600 lbs test, 44' slings w/ eyes	I & I Slings	EE1-908	3	310.00	930.00
Concrete, Labour and transport						
Concrete, Labour and transport		American Conc.				5,350.00
Addl Labour						1,350.00
Totals						
Total cost						12,085.44
Already Paid						2,025.00
Upcoming Cost						10,060.44